A chemical screen based on an interruption of zebrafish gastrulation identifies the HTR2C inhibitor Pizotifen as a suppressor of EMT-mediated metastasis

Joji Nakayama[1,2,3,4,§], Lora Tan[1], Boon Cher Goh[2], Shu Wang[1, 5], Hideki Makinoshima[3,6] and Zhiyuan Gong[1,§]

[1]Department of Biological Science, National University of Singapore, Singapore
[2]Cancer Science Institute of Singapore, National University of Singapore, Singapore
[3]Tsuruoka Metabolomics Laboratory, National Cancer Center, Tsuruoka, Japan
[4]Shonai Regional Industry Promotion Center, Tsuruoka, Japan.
[5]Institute of Bioengineering and Nanotechnology, Singapore
[6]Division of Translational Research, Exploratory Oncology Research and Clinical Trial Center, National Cancer Center, Kashiwa, Japan.

[§]Corresponding authors:
Joji Nakayama
email: Zmetastasis@gmail.com

Zhiyuan Gong
email: dbsgzy@nus.edu.sg

Keywords: Metastasis, gastrulation, EMT, Phenotyping screening, zebrafish

Total words excluding supplemental figure legends and references section: 5468

Number of figures: 5
Number of tables: 1
Number of supplemental figures: 3
Number of supplemental tables: 6

Abstract

Metastasis is responsible for approximately 90% of cancer-associated mortality but few models exist that allow for rapid and effective screening of anti-metastasis drugs. Current mouse models of metastasis are too expensive and time consuming to use for rapid and high-throughput screening. Therefore, we created a unique screening concept utilizing conserved mechanisms between zebrafish gastrulation and cancer metastasis for identification of potential anti-metastatic drugs. We hypothesized that small chemicals that interrupt zebrafish gastrulation might also suppress metastatic progression of cancer cells and developed a phenotype-based chemical screen to test the hypothesis. The screen used epiboly, the first morphogenetic movement in gastrulation, as a marker and enabled 100 chemicals to be tested in five hours. The screen tested 1280 FDA-approved drugs and identified Pizotifen, an antagonist for serotonin receptor 2C (HTR2C) as an epiboly-interrupting drug. Pharmacologic and genetic inhibition of HTR2C suppressed metastatic progression in a mouse model. Blocking HTR2C with Pizotifen restored epithelial properties to metastatic cells through inhibition of Wnt-signaling. In contrast, HTR2C induced epithelial to mesenchymal transition (EMT) through activation of Wnt-signaling and promoted metastatic dissemination of human cancer cells in a zebrafish xenotransplantation model. Taken together, our concept offers a novel platform for discovery of anti-metastasis drugs.

Introduction

Metastasis, a leading contributor to the morbidity of cancer patients, occurs through multiple steps: invasion, intravasation, extravasation, colonization, and metastatic tumor formation (1-3). The physical translocation of cancer cells is an initial step of metastasis and molecular mechanisms of it involve cell motility, the breakdown of local basement membrane, loss of cell polarity, acquisition of stem cell-like properties, and EMT (4-6). These cell-biological phenomena are also observed during vertebrate gastrulation in that evolutionarily conserved morphogenetic movements of epiboly, internalization, convergence, and extension progress (7). In zebrafish, the first morphogenetic movement, epiboly, is initiated at approximately 4 hours post fertilization (hpf) to move cells from the animal pole to eventually engulf the entire yolk cell by 10 hpf (8, 9). The embryonic cell movements are governed by the molecular mechanisms that are partially shared in metastatic cell dissemination.

At least fifty common genes were shown to be involved in both metastasis and gastrulation progression: Knockdown of these genes in Xenopus or zebrafish induced gastrulation defects; conversely, overexpression of these genes conferred metastatic potential on cancer cells and knockdown of these genes suppressed metastasis (Table S1). This evidence led us to hypothesize that small molecules that interrupt zebrafish gastrulation may suppress metastatic progression of human cancer cells.

Here we report a unique screening concept based on the hypothesis. Pizotifen, an antagonist for HTR2C, was identified from the screen as a “hit” that interrupted zebrafish gastrulation. A mouse model of metastasis confirmed pharmacological and genetic inhibition of HTR2C suppressed metastatic progression. Moreover, HTR2C induced EMT and promoted metastatic dissemination of non-metastatic cancer cells in a zebrafish xenotransplantation model. These results demonstrated that this concept could offer a novel high-throughput platform for discovery of anti-metastasis drugs and can be converted to a chemical genetic screening platform.

Results

Small molecules interrupting epiboly of zebrafish have a potential to suppress metastatic progression of human cancer cells.

Before performing a screening assay, we conducted preliminary experiments to test the hypothesis. First, we examined whether hindering the molecular function of reported genes, whose knockdown induced gastrulation defects in zebrafish, might suppress cell motility and invasion of cancer cells. We chose protein arginine methyltransferase 1 (PRMT1) and cytochrome P450 family 11 (CYP11A1), both of whose knockdown induced gastrulation defects in zebrafish but whose involvement in metastatic progression is unclear (10, 11). Elevated expression of PRMT1 and CYP11A1 were observed in highly metastatic human breast cancer cell lines and knockdown of these genes through RNA interference suppressed the motility and invasion of MDA-MB-231 cells without affecting their viability (Figure S1A-C).

Next, we conducted an inverse examination of whether chemicals which were reported to suppress metastatic dissemination of cancer cells could interrupt epiboly progression of zebrafish embryos. Niclosamide and Vinpocetine are reported to suppress metastatic progression (12, 13) (14, 15). Either Niclosamide or Vinpocetine-treated zebrafish embryos showed complete arrest at very early stages or severe delay in epiboly progression, respectively (Figure S1D).

These results suggest that epiboly could serve as a marker for this screening assay and epiboly-interrupting drugs that are identified through this screening could have the potential to suppress metastatic progression of human cancer cells.

132 FDA-approved drugs induced delayed in epiboly of zebrafish embryos

We screened 1,280 FDA, EMA or other agencies-approved drugs (Prestwick, Inc) in our zebrafish assay. The screening showed that 0.9% (12/1280) of the drugs, including Actimycin A and Tolcapone, induced severe or complete arrest of embryonic cell

102 movement when embryos were treated with 10μM. 5.2% (66/1280) of the drugs, such as
103 Dicumarol, Racecadotril, Pizotifen and S(-) Eticlopride hydrochloride, induced either
104 delayed epiboly or interrupted epiboly of the embryos. 93.3% (1194/1280) of drugs has
105 no effect on epiboly progression of the embryos. 0.6% (8/1280) of drugs induced a toxic
106 lethality. Epiboly progression was affected more severely when embryos were treated
107 with 50μM; 1.7% (22/1280) of the drugs induced severe or complete arrest of it. 8.6%
108 (110/1280) of the drugs induced either delayed epiboly or interrupt epiboly of the
109 embryos. 4.3% (55/1280) of drugs induced a toxic lethality (Figure 1A and 1B, Table S2).
110 Among the epiboly-interrupting drugs, several drugs have already been reported to inhibit
111 metastasis-related molecular mechanisms: Adrenosterone or Zardaverine, which target
112 HSD11β1 or PDE3 and 4, respectively, are reported to inhibit EMT (16, 17);
113 Racecadotril, which targets enkephalinase, is reported to confer metastatic potential on
114 colon cancer cell (18); and Disulfiram, which targets ALDH, is reported to confer stem-
115 like properties on metastatic cancer cells (19). This evidence suggests that epiboly-
116 interrupting drugs have the potential for suppressing metastasis of human cancer cells.
117
118 **Identified drugs suppressed cell motility and invasion of human cancer cells.**
119 It has been reported that zebrafish have orthologues to 86% of 1318 human drug targets
120 (20). However, it was not known whether the epiboly-interrupting drugs could suppress
121 metastatic dissemination of human cancer cells. To test this, we subjected the 78 epiboly-
122 interrupting drugs that showed a suppressor effect on epiboly progression at a 10μM
123 concentration to *in vitro* experiments using a human cancer cell line. The experiments
124 examined whether the drugs could suppress cell motility and invasion of MDA-MB-231
125 cells through a Boyden chamber. Before conducting the experiment, we investigated
126 whether these drugs might effect viability of MDA-MB-231 cells using an MTT assay.
127 Sixteen of the 78 drugs strongly effected cell viability at concentrations less than 1μM
128 and were not used in the cell motility experiments. The remaining 62 drugs were assayed

129 in Boyden chamber motility experiments. Twenty of the 62 drugs inhibited cell motility
130 and invasion of MDA-MB-231 cells without effecting cell viability. Among the 20 drugs,
131 Hexachlorophene and Nitazoxanide were removed since the primary targets of the drugs,
132 D-lactate dehydrogenase and pyruvate ferredoxin oxidoreductase are not expressed in
133 mammalian cells. With the exception of Ipriflavone, whose target is still unclear, the
134 known primary targets of the remaining 17 drugs are reported to be expressed by
135 mammalian cells (Figure 2A and Table 1).
136 We confirmed if highly metastatic human cancer cell lines expressed the genes
137 that code for these targets using Western blotting analyses. Among the genes, serotonin
138 receptor 2C (HTR2C), which is a primary target of Pizotifen, was highly expressed in
139 only metastatic cell lines (Figure 2B). Pizotifen suppressed cell motility and invasion of
140 several highly metastatic human cancer cell lines in a dose-dependent manner (Figure
141 2C). Similarly, Dopamine receptor D2 (DRD2), which is a primary target of S(-)
142 Eticlopride hydrochloride, was highly expressed in only metastatic cell lines, and the drug
143 suppressed cell motility and invasion of these cells in a dose-dependent manner (Figure
144 S2).
145 These results indicate that a number of the epiboly-interrupting drugs also have
146 suppressor effects on cell motility and invasion of highly metastatic human cancer cells.
147
148 **Pizotifen suppressed metastatic dissemination of human cancer cells in a zebrafish**
149 **xenotransplantation model.**
150 While a number of the epiboly-interrupting drugs suppressed cell motility and invasion of
151 human cell lines *in vitro,* it was still unclear whether the drugs could suppress metastatic
152 dissemination of cancer cells in vivo. Therefore, we examined whether the identified
153 drugs could suppress metastatic dissemination of these human cancer cells in a zebrafish
154 xenotransplantation model. Pizotifen was selected to test since HTR2C was overexpressed
155 only in highly metastatic cell lines supporting the hypothesis that it could be a novel target

156 for blocking metastatic dissemination of cancer cells (Figure 2B). Red fluorescent
157 protein-labelled MDA-MB-231 (231R) cells were injected into the duct of Cuvier of *Tg*
158 *(kdrl:eGFP)* zebrafish at 2 dpf and then maintained in the presence of either vehicle or
159 Pizotifen. Twenty-four hours post-injection, the numbers of fish showing metastatic
160 dissemination of 231R cells were measured via fluorescence microscopy. In this model,
161 the dissemination patterns were generally divided into three categories: (i) head
162 dissemination, in which disseminated 231R cells exist in the vessel of the head part; (ii)
163 trunk dissemination, in which the cells were observed in the vessel dilating from the trunk
164 to the tail; (iii) end-tail dissemination, in which the cells were observed in the vessel of
165 the end-tail part (16).

166 Three independent experiments revealed that the frequencies of fish in the drug-
167 treated group showing head, trunk, or end-tail dissemination, significantly decreased to
168 55.3±7.5%, 28.5±5.0% or 43.5±19.1% when compared with those in the vehicle-treated
169 group; 95.8±5.8%, 47.1±7.7% or 82.6±12.7%. Conversely, the frequency of the fish in the
170 drug-treated group not showing any dissemination, significantly increased to 45.4±0.5%
171 when compared with those in the vehicle-treated group; 2.0±2.9% (Figure 2D and Table
172 S3).

173 Similar effects were observed in another xenograft experiments using an RFP-
174 labelled human pancreatic cancer cell line, MIA-PaCa-2 (MP2R). In the drug treated
175 group, the frequencies of the fish showing head, trunk or end-tail dissemination,
176 significantly decreased to 15.3±6.7%, 6.2±1.3%, or 41.1±1.5%; conversely, the frequency
177 of the fish not showing any dissemination significantly increased to 46.3±8.9% when
178 compared with those in the vehicle-treated group; 74.5±11.1%, 18.9±14.9%, 77.0±9.0%,
179 or 17.2±0.7% (Figure S3 and Table S4).

180 To eliminate the possibility that the metastasis suppressing effects of Pizotifen
181 might result from off-target effects of the drug, we conducted validation experiments to
182 determine whether knockdown of HTR2C would show the same effects. Sub-clones of

183 231R cells that expressed shRNA targeting either LacZ or HTR2C were injected into the
184 fish at 2 dpf and the fish were maintained in the absence of drug. In the fish that were
185 inoculated with shHTR2C 231R cells, the frequencies of the fish showing head, trunk,
186 and end-tail dissemination, significantly decreased to 6.7±4.9%, 6.7±0.7%, or
187 20.0±16.5%; conversely, the frequency of the fish not showing any dissemination,
188 significantly increased to 80.0±4.4% when compared with those that were inoculated with
189 shLacZ 231R cells; 80.0±27.1%, 20.0±4.5%, 90.0± 7.7%, or 0% (Figure 2E and Table
190 S5).
191 These results indicate that pharmacological and genetic inhibition of HTR2C
192 suppressed metastatic dissemination of human cancer cells in vivo.
193
194 **Pizotifen suppressed metastasis progression of a mouse model of metastasis.**
195 We examined the metastasis-suppressor effect of Pizotifen in a mouse model of
196 metastasis (21). Luciferase-expressing 4T1 murine mammary carcinoma cells were
197 inoculated into the mammary fat pads (MFP) of female BALB/c mice. On day two post
198 inoculation, the mice were randomly assigned to two groups and one group received once
199 daily intraperitoneal injections of 10mg/kg Pizotifen while the other group received a
200 vehicle injection. Bioluminescence imaging and tumor measurement revealed that the
201 sizes of the primary tumors in Pizotifen-treated mice were equal to those in the vehicle-
202 treated mice at the time of resection on day 10 post inoculation. Immunofluorescent
203 staining also demonstrated that the percentage of Ki67 positive cells in the resected
204 primary tumors of Pizotifen-treated mice were the same as those of vehicle-treated mice
205 (Figure 3A-C), additionally, both groups showed less than 1% cleaved caspase 3 positive
206 cells (data not shown). Therefore, no anti-tumor effect of Pizotifen was observed on the
207 primary tumor. After 70 days from inoculation, bioluminescence imaging detected light
208 emitted in the lungs, livers and lymph nodes of vehicle-treated mice but not those of
209 Pizotifen-treated mice (Figure 3C). Vehicle-treated mice formed 5 to 50 metastatic

210 nodules per lung in all 10 mice analyzed; conversely, Pizotifen-treated mice (n=10)
211 formed 0 to 5 nodules per lung in all 10 mice analyzed (Figure 3D). Histological analyses
212 confirmed that metastatic lesions in the lungs were detected in all vehicle-treated mice;
213 conversely, they were detected in only 2 of 10 Pizotifen-treated mice and the rest of the
214 mice showed metastatic colony formations around the bronchiole of the lung. In addition,
215 4 of 10 vehicle-treated mice exhibited metastasis in the liver and the rest showed
216 metastatic colony formation around the portal tract of the liver. In contrast, none of 10
217 Pizotifen-treated mice showed liver metastases and only half of the 10 mice showed
218 metastatic colony formation around the portal tract (Figure 3E). These results indicate that
219 Pizotifen can suppress metastasis progression without affecting primary tumor growth.
220 To eliminate the possibility that the metastasis suppressing effects of Pizotifen
221 might result from off-target effects, we conducted validation experiments to determine
222 whether knockdown of HTR2C would show the same effects. The basic experimental
223 process followed the experimental design described above except that sub-clones of 4T1
224 cells that expressed shRNA targeting either LacZ or HTR2C were injected into the MFP
225 of female BALB/c mice and the mice were maintained without drug. Histological
226 analyses revealed that all of the mice (n=5) that were inoculated with 4T1 cells expressing
227 shRNA targeting LacZ showed metastases in the lungs. The mean number of metastatic
228 lesions in a lung was 26.4±7.8. In contrast, only one of the mice (n=5) were inoculated
229 with 4T1 cells expressing shRNA targeting HTR2C showed metastases in the lungs and
230 the rest of the mice showed metastatic colony formation around the bronchiole of the
231 lung. The mean number of metastatic lesions in the lung significantly decreased to 10% of
232 those of mice that were inoculated with 4T1 cells expressing shRNA targeting LacZ
233 (Figure 3F-H).
234 Taken together, pharmacological and genetic inhibition of HTR2C showed an
235 anti-metastatic effect in the 4T1 model system.
236

237 **HTR2C promoted EMT-mediated metastatic dissemination of human cancer cells**

238 Although pharmacological and genetic inhibition of HTR2C inhibited metastasis
239 progression, a role for HTR2C on metastatic progression has not been reported.
240 Therefore, we examined whether HTR2C could confer metastatic properties on poorly
241 metastatic cells.

242 Firstly, we established a stable sub-clone of MCF7 human breast cancer cells
243 expressing either vector control or HTR2C. Vector control expressing MCF7 cells
244 maintained highly organized cell-cell adhesion and cell polarity; however, HTR2C-
245 expressing MCF7 cells led to loss of cell-cell contact and cell scattering. The cobblestone-
246 like appearance of these cells was replaced by a spindle-like, fibroblastic morphology.
247 Western blotting and immunofluorescence (IF) analyses revealed that HTR2C-expressing
248 MCF7 cells showed loss of E-cadherin and EpCAM, and elevated expressions of N-
249 cadherin, vimentin and an EMT-inducible transcriptional factor Zeb1. Similar effects
250 were validated through another experiment using an immortal keratinocyte cell line,
251 HaCaT cells, in that HTR2C-expressing HaCaT cells also showed loss of cell-cell contact
252 and cell scattering with loss of epithelial markers and gain of mesenchymal markers
253 (Figure 4A-C). Therefore, both the morphological and molecular changes in the HTR2C-
254 expressing MCF7 and HaCaT cells demonstrated that these cells had undergone an EMT.

255 Next, we examined whether HTR2C-driven EMT could promote metastatic
256 dissemination of human cancer cells. Boyden chamber assay revealed that HTR2C
257 expressing MCF7 cells showed an increased cell motility and invasion compared with
258 vector control-expressing MCF7 cells in vitro (Figure 4D). Moreover, we conducted in
259 vivo examination of whether HTR2C expression could promote metastatic dissemination
260 of human cancer cells in a zebrafish xenotransplantation model. Red fluorescence protein-
261 labelled MCF7 cells expressing either vector control or HTR2C were injected into the
262 duct of Cuvier of *Tg* (*kdrl:eGFP*) zebrafish at 2 dpf. Twenty-four hours post injection, the
263 frequencies of the fish showing metastatic dissemination of the inoculated cells were

264 measured using fluorescence microscopy. In the fish that were inoculated with HTR2C
265 expressing MCF7 cells, the frequencies of the fish showing head, trunk, and end-tail
266 dissemination significantly increased to 96.7±4.7%, 68.8±6.4%, or 89.5±3.4%;
267 conversely, the frequency of the fish not showing any dissemination decreased to 0%
268 when compared with those in the fish that were inoculated with vector control expressing
269 MCF7 cells; 33.1±18.5%, 0%, 56.9± 4.4%, or 43% (Figure 4E and Table S6).
270 These results indicated that HTR2C promoted metastatic dissemination of cancer
271 cells though induction of EMT, and suggest that the screen can easily be converted to a
272 chemical genetic screening platform.
273
274 **Pizotifen induced mesenchymal to epithelial transition through inhibition of Wnt-**
275 **signaling.**
276 Finally, we elucidated the mechanism of action of how Pizotifen suppressed metastasis,
277 especially metastatic dissemination of cancer cells. Our results showed that HTR2C
278 induced EMT and that pharmacological and genetic inhibition of HTR2C suppressed
279 metastatic dissemination of MDA-MB-231 cells that had already transitioned to
280 mesenchymal-like traits via EMT. Therefore, we speculated that blocking HTR2C with
281 Pizotifen might inhibit the molecular mechanisms which follow EMT induction. We
282 firstly investigated the expressions of epithelial and mesenchymal markers in Pizotifen-
283 treated MDA-MB-231 cells since the activation of an EMT program needs to be transient
284 and reversible, and transition from a fully mesenchymal phenotype to a epithelial-
285 mesenchymal hybrid state or a fully epithelial phenotype is associated with malignant
286 phenotypes (22). IF and FACS analyses revealed 20% of Pizotifen-treated MDA-MB-231
287 cells restored E-cadherin expression. Also, western blotting analysis demonstrated that
288 4T1 primary tumors from Pizotifen-treated mice has elevated E-cadherin expression
289 compared with tumors from vehicle-treated mice (Figure 5A-C). However, mesenchymal
290 markers did not change between vehicle and Pizotifen-treated MDA-MB-231 cells (data

291 not shown). We further analyzed E-cadherin positive (E-cad$^+$) cells in Pizotifen-treated
292 MDA-MB-231 cells. The E-cad$^+$ cells showed elevated expressions of epithelial markers
293 KRT14 and KRT19; and decreased expression of mesenchymal makers vimentin, MMP1,
294 MMP3, and S100A4. Recent research reports that an EMT program needs to be transient
295 and reversible and that a mesenchymal phenotype in cancer cells is achieved by
296 constitutive ectopic expression of Zeb1. In accordance with the research, the E-cad$^+$ cells
297 and 4T1 primary tumors from Pizotifen-treated mice had decreased Zeb1 expression
298 compared with vehicle-treated cells and tumors from vehicle-treated mice (Figure 5D). In
299 contrast, HTR2C-expressing MCF7 and HuMEC cells expressed Zeb1 but not vehicle
300 control MCF7 and HuMEC cells (Figure 4C). These results indicate that HTR2C-
301 mediated signaling induced EMT through up-regulation of Zeb1 and blocking HTR2C
302 with Pizotifen induced mesenchymal to epithelial transition through downregulation of
303 Zeb1.

304 We further investigated the mechanism of action of how blocking HTR2C with
305 Pizotifen induced down-regulation of Zeb1. In embryogenesis, serotonin-mediated
306 signaling is required for Wnt-dependent specification of the superficial mesoderm during
307 gastrulation (23). In cancer cells, overexpression of HTR1D is associated with Wnt-
308 signaling which enables induction of EMT (24, 25). This evidence led to a hypothesis that
309 HTR2C-mediated signaling might turn on transcriptional activity of β-catenin and that
310 might induce up-regulation of EMT-TFs. IF analyses revealed β-catenin was accumulated
311 in the nucleus of HTR2C-expressing MCF7 cells but it was located in the cytoplasm of
312 vector control-expressing cells (Figure 5E). Nuclear accumulation of β-catenin in
313 HTR2C-expressing MCF7 cells was confirmed by western blot (Figure 5F). In contrast,
314 Pizotifen-treated MDA-MB-231 cells showed β-catenin located in the cytoplasm of the
315 cells. Vehicle-treated cells showed β-catenin accumulated in the nucleus of the cells.
316 (Figure 5G), and western blotting analysis confirmed that it was located in the cytoplasm
317 of Pizotifen-treated MDA-MB-231 cells (Figure 5H). Furthermore,

318 immunohistochemistry and western blotting analyses showed that β-catenin accumulated
319 in the nucleus, and phospho-GSKβ and Zeb1 expression were decreased in 4T1 primary
320 tumors from Pizotifen-treated mice compared with vehicle-treated mice (Figure 5C).
321 These results indicated that HTR2C would regulate transcriptional activity of β-catenin
322 and Pizotifen could inhibit it.
323 Taken together, we conclude that blocking HTR2C with Pizotifen restored
324 epithelial properties to metastatic cells (MDA-MB-231 and 4T1 cells) through a decrease
325 of transcriptional activity of β-catenin and that suppressed metastatic progression of the
326 cells.
327

328 **Figures and figure legends**

329 **Figure 1**

330

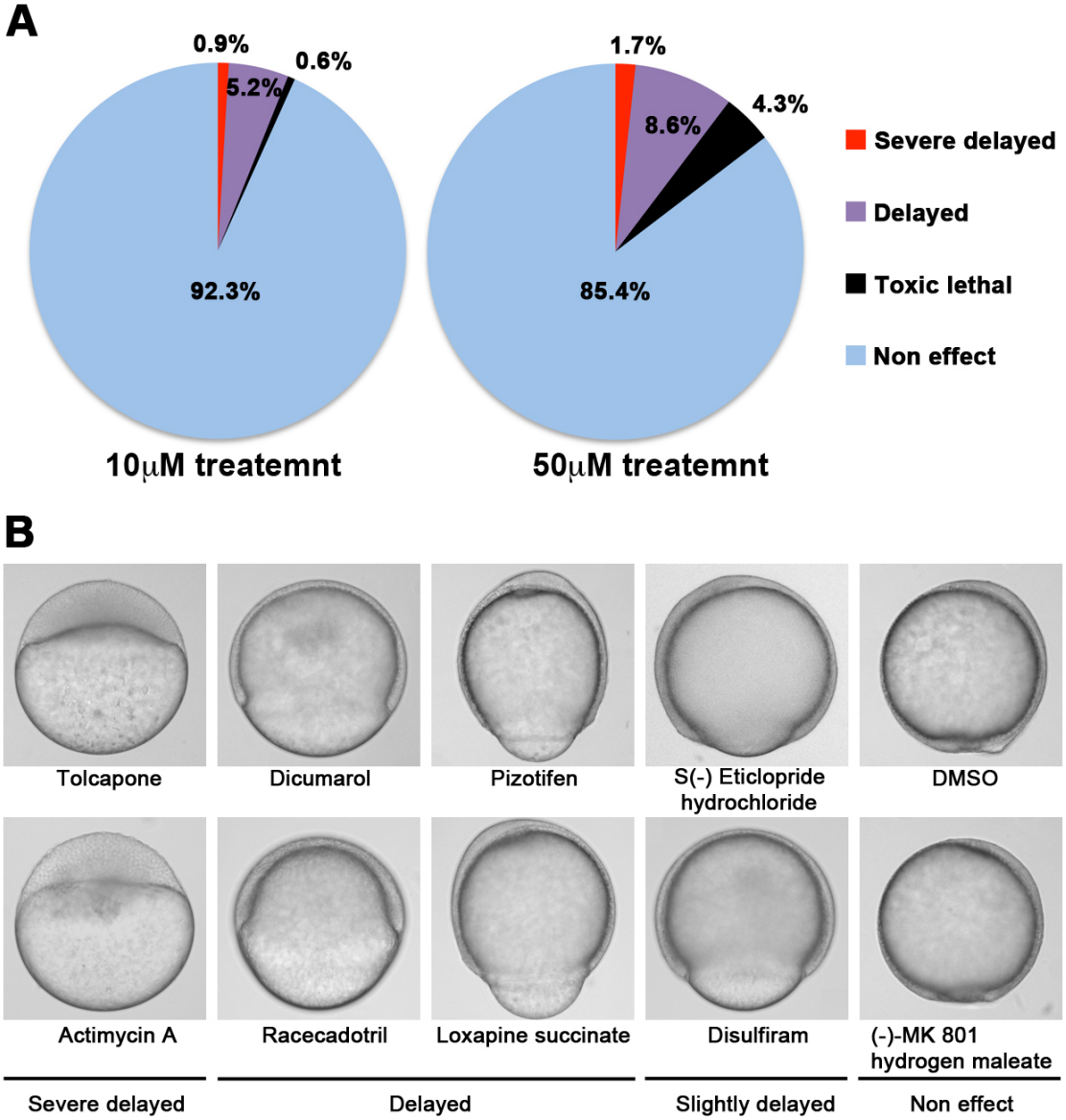

331

332

333 **Figure 1. A chemical screen for identification of epiboly-interrupting drugs.**

334 (A) Cumulative results of the chemical screen in which each drug was used at either

335 10μM (left) or 50μM (right) concentrations. 1,280 FDA, EMA or other agencies-

336 approved drugs were subjected to this screening. Positive "hit" drugs were those that

337 interrupted epiboly progression. (B) Representative samples of the embryos that were

338 treated with indicated drugs.

339 **Figure 2**

340

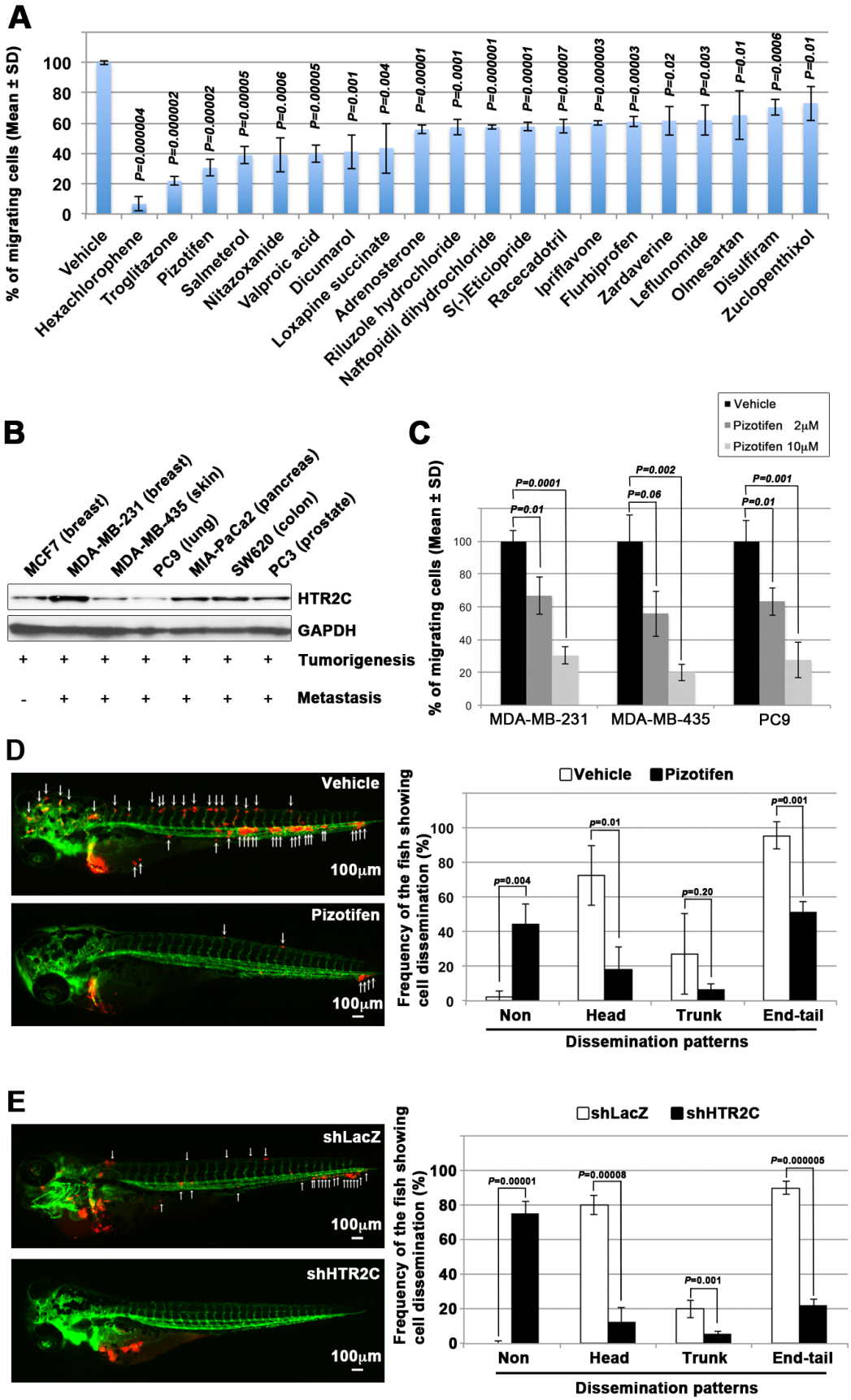

341

342 **Figure 2. Pizotifen, one of epiboly-interrupting drugs suppressed metastatic**

343 **dissemination of human cancer cells lines in vivo and vitro.**

344 (A) Effect of the epiboly-interrupting drugs on cell motility and invasion of MBA-MB-
345 231 cells. MBA-MB-231 cells were treated with vehicle or each of the epiboly-
346 interrupting drugs and then subjected to Boyden chamber assays. Fetal bovine serum
347 (1%v/v) was used as the chemoattractant in both assays. Each experiment was performed
348 at least twice. (B) Western blot analysis of HTR2C levels (top) in a non-metastatic human
349 cancer cell line, MCF7 (breast) and highly metastatic human cancer cell lines, MDA-MB-
350 231 (breast), MDA-MB-435 (melanoma), PC9 (lung), MIA-PaCa2 (pancreas), PC3
351 (prostate) and SW620 (colon); GAPDH loading control is shown (bottom). (C) Effect of
352 pizotifen on cell motility and invasion of MBA-MB-231, MDA-MB-435 and PC9 cells.
353 Either vehicle or pizotifen treated the cells were subjected to Boyden chamber assays.
354 Fetal bovine serum (1%v/v) was used as the chemoattractant in both assays. Each
355 experiment was performed at least twice. (D) and (E) Representative images of
356 dissemination of 231R, shLacZ 231R or shHTR2C 231R cells in zebrafish
357 xenotransplantation model. The fish larvae that were inoculated with 231R cells, were
358 treated with either vehicle (top left) or the drug (lower left) (D). The fish larvae that were
359 inoculated with either shLacZ 231R or shHTR2C 231R cells (lower left) (E). White
360 arrows head indicate disseminated 231R cells. The images were shown in 4x
361 magnification. Scale bar, 100μm. The mean frequencies of the fish showing head, trunk,
362 or end-tail dissemination were counted (graph on right). Each value is indicated as the
363 mean ± SEM of two independent experiments. Statistical analysis was determined by
364 Student's t test. See also Figure S2 and S3, Table S3-S5.
365

366 **Figure 3**

367

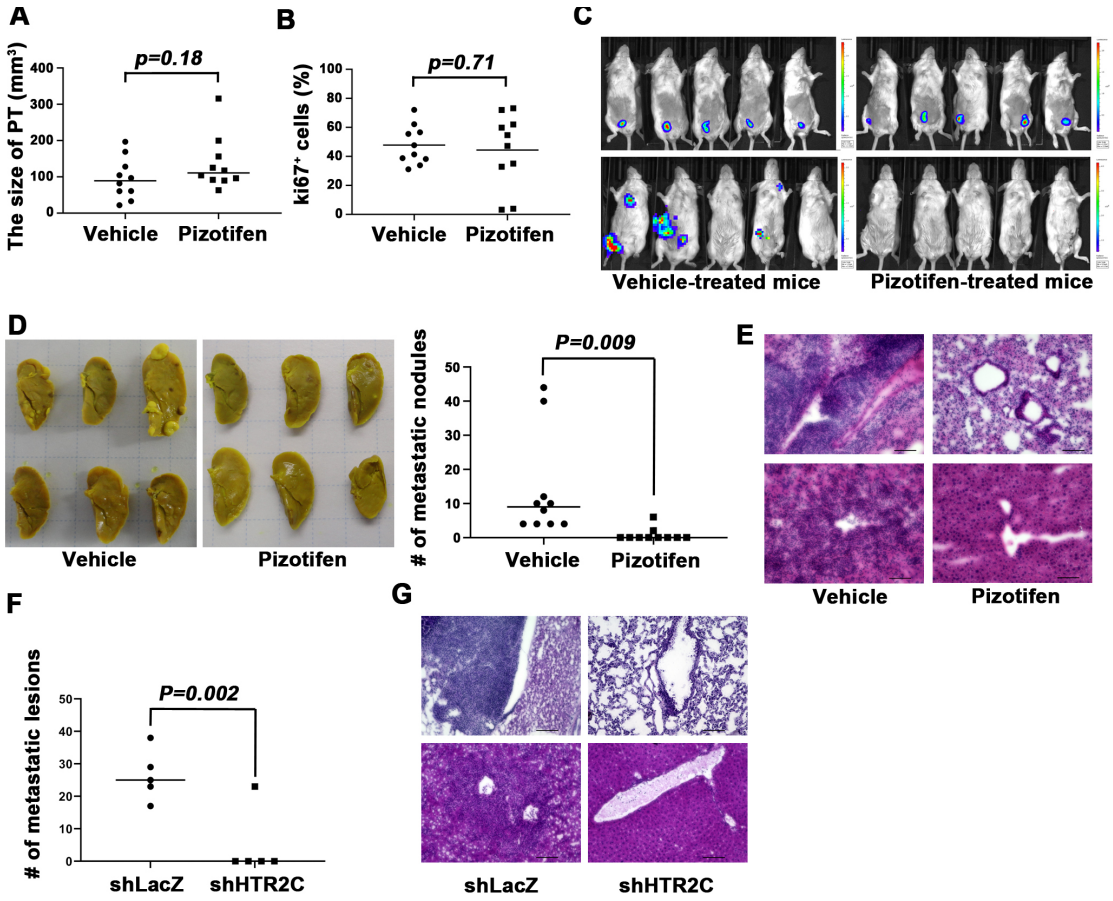

368

369

370 **Figure 3. Pizotifen suppressed metastatic progression in a mouse model of**

371 **metastasis.**

372 (A) Mean volumes (n=10 per group) of 4T1 primary tumors formed in the mammary fat

373 pad of either vehicle or Pizotifen-treated mice at day 10 post injection. (B) Ki67

374 expression level in 4T1 primary tumors formed in the mammary fat pad of either vehicle

375 or Pizotifen-treated mice at day 10 post injection. The mean expression levels of Ki67

376 (n=10 mice per group) were determined and were calculated as the mean ration of Ki67

377 positive cells to DAPI area. (C) Representative images of primary tumors on day 10 post

378 injection (top panels) and metastatic burden on day 70 post injection (bottom panels)

379 taken using an IVIS Imaging System. (D) Representative images of the lungs from either

380 vehicle (top) or Pizotifen-treated mice (bottom) at 70 days past tumor inoculation.

381 Number of metastatic nodules in the lung of either vehicle or Pizotifen-treated mice
382 (right). (E) Representative H&E staining of the lung (top) and liver (bottom) from either
383 vehicle or Pizotifen-treated mice. (F) The mean number of metastatic lesions in step
384 sections of the lungs from the mice that were inoculated with 4T1-12B cells expressing
385 shRNA targeting for either LacZ or HTR2C. (G) Representative H&E staining of the lung
386 and liver from the mice that were inoculated with 4T1-12B cells expressing shRNA
387 targeting for either LacZ or HTR2C. Each value is indicated as the mean ± SEM.
388 Statistical analysis was determined by Student's *t* test.
389

390 **Figure 4**

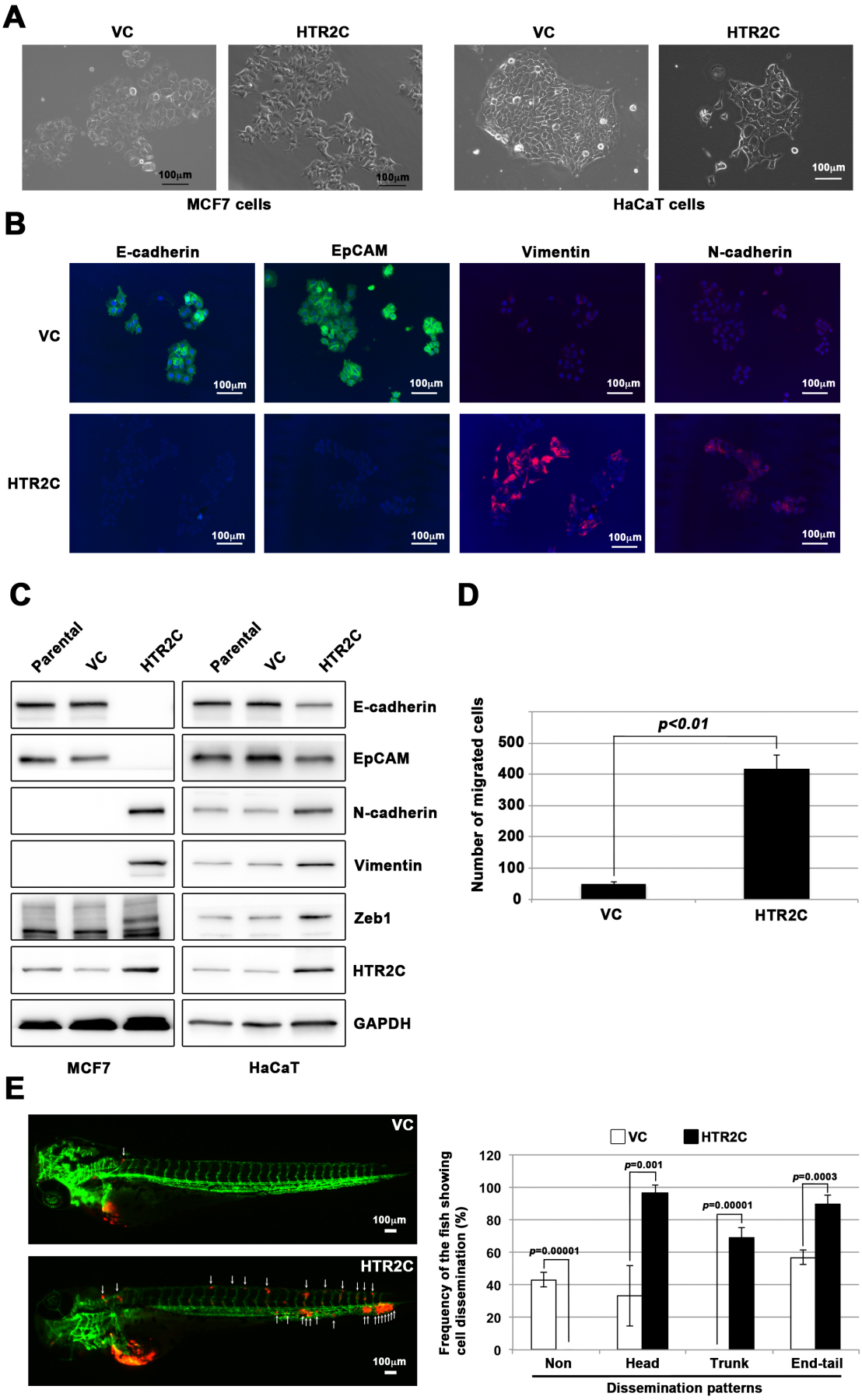

391

392 **Figure 4. HTR2C induced EMT-mediated metastatic dissemination of human cancer**
393 **cells.**
394 (A) The morphologies of the MCF7 and HaCaT cells expressing either the control vector
395 or HTR2C were revealed by phase contrast microscopy. (B) Immunofluorescence staining
396 of E-cadherin, EpCAM, Vimentin, and N-cadherin expressions in the MCF7 cells from
397 Figure 4A. (C) Expression of E-cadherin, EpCAM, Vimentin, N-cadherin, and HTR2C
398 was examined by western-blotting in the MCF7 and HaCaT cells; GAPDH loading
399 control is shown (bottom). (D) Effect of HTR2C on cell motility and invasion of MCF7
400 cells. MCF7 cells were subjected to Boyden chamber assays. Fetal bovine serum (1%v/v)
401 was used as the chemoattractant in both assays. Each experiment was performed at least
402 twice. (E) Representative images of dissemination patterns of MCF7 cells expressing
403 either the control vector (top left) or HTR2C (lower left) in a zebrafish
404 xenotransplantation model. White arrows head indicate disseminated MCF7 cells. The
405 mean frequencies of the fish showing head, trunk, or end-tail dissemination tabulated
406 (right). Each value is indicated as the mean ± SEM of two independent experiments.
407 Statistical analysis was determined by Student's *t* test.
408 See also Table S6.

409 **Figure 5**

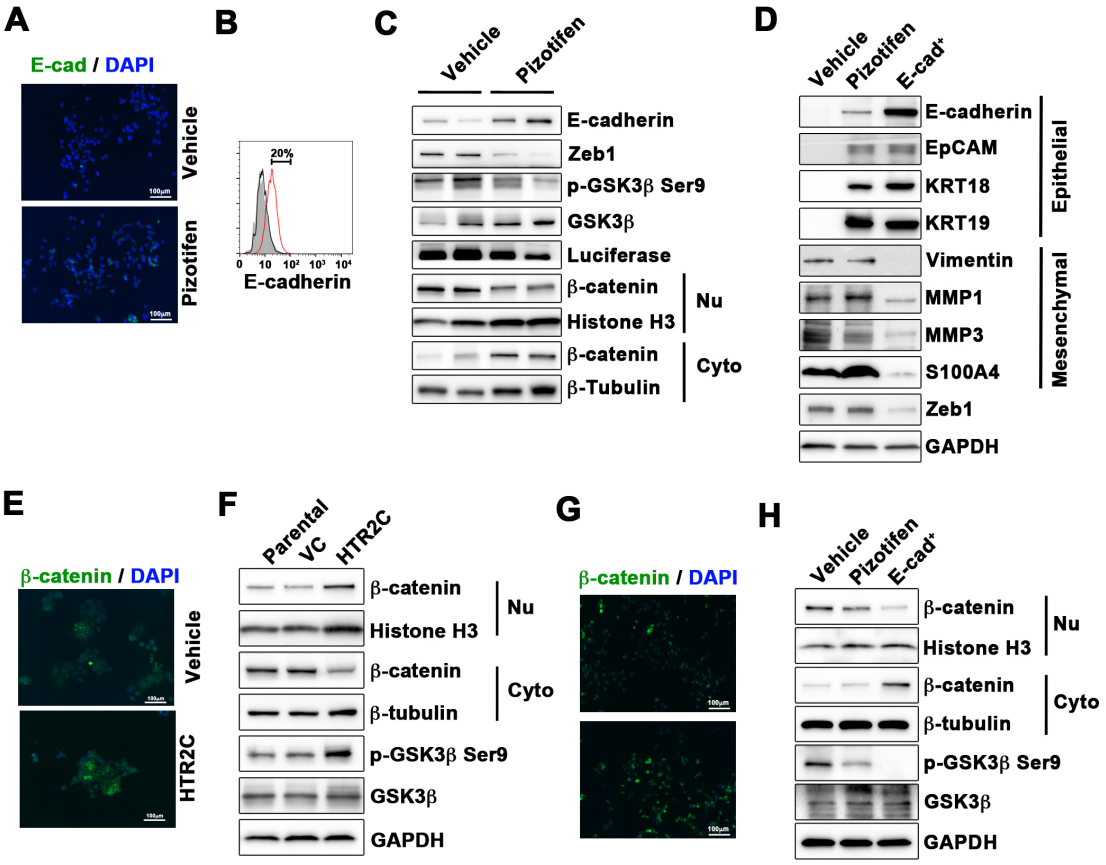

410

411 **Figure 5. Pizotifen restored mesenchymal-like traits of MDA-MB-231 cells into**

412 **epithelial traits through blocking nuclear accumulation of β-catenin.**

413 (A) IF staining of E-cadherin in either vehicle or Pizotifen-treated MDA-MB-231 cells.

414 (B) Surface expression of E-cadherin in either vehicle (black) or Pizotifen (red)-treated

415 MDA-MB-231 cells by FACS analysis. Non-stained controls are shown in gray. (C)

416 Protein expressions levels of E-cadherin, Zeb1, and β-catenin in the cytoplasm and

417 nucleus of 4T1 primary tumors from either vehicle or Pizotifen-treated mice are shown;

418 Luciferase, Histone H3, and β-tubulin are used as loading control for whole cell, nuclear

419 or cytoplasmic lysate, respectively. (D) Protein expression levels of epithelial and

420 mesenchymal markers and Zeb1 in either vehicle or Pizotifen-treated MDA-MB-231 cells

421 or E-cadherin positive (E-cad^{+}) cells in Pizotifen-treated MDA-MB-231 cells are shown.

422 (E) Immunofluorescence staining of β-catenin in the MCF7 cells expressing either vector

423 control or HTR2C. (F) Expressions of β-catenin in the cytoplasm and nucleus of MCF7

424 cells. (G) IF staining of β-catenin in either vehicle or Pizotifen-treated MDA-MB-231

425 cells. (H) Expressions of β-catenin in the cytoplasm and nucleus of MDA-MB-231 cells

426 and the E-cad^{+} cells.

427

428 **Table 1. Primary targets of the identified drugs**

429

The identified drugs	Primary targets of the identified drugs
Hexachlorophene	D-lactate dehydrogenase (D-LDH), not expressed in mammalian cells
Troglitazone	Agonist for Peroxisome proliferator-activated receptor α and γ (PPARα and γ)
Pizotifen malate	5-hydroxytryptamine receptor 2C (HTR2C)
Salmeterol	Adrenergic receptor beta 2 (ADRB2)
Nitazoxanide	Pyruvate ferredoxin oxidoreductase (PFOR), not expressed in mammalian cells
Valproic acid	Histone deacetylases (HDACs)
Dicumarol	NAD(P)H dehydrogenase quinone 1 (NQO1)
Loxapine succinate	Dopamine receptor D2 and D4 (DRD2 and DRD4)
Adrenosterone	Hydroxysteroid (11-beta) dehydrogenase 1 (HSD11β1)
Riluzole hydrochloride	Glutamate R and Voltage-dependent Na+ channel
Naftopidil dihydrochloride	5-hydroxytryptamine receptor 1A (HTR1A) and α1-adrenergic receptor (AR)
S(-)Eticlopride hydrochloride	Dopamine receptor D2 (DRD2)
Racecadotril	Membrane metallo-endopeptidase (MME)
Ipriflavone	Unknow
Flurbiprofen	Cyclooxygenase 1 and 2 (Cox1 and 2)
Zardaverine	Phosphodiesterase III/IV (PDE3/4)
Leflunomide	Dihydroorotate dehydrogenase (DHODH)
Olmesartan	Angiotensin II receptor alpha
Disulfiram	Aldehyde dehydrogenase (ALDH) Dopamine β-hydroxylase (DBH)
Zuclopenthixol dihydrochloride	Dopamine receptors D1 and D2 (DRD1 and 2)

430

431 **Discussion**

432 Reducing or eliminating mortality associated with metastatic disease is a key goal of
433 medical oncology, but few models exist that allow for rapid, effective screening of novel
434 compounds that target the metastatic dissemination of cancer cells. Based on accumulated

435 evidence that at least fifty genes play an essential role in governing both metastasis and
436 gastrulation progression (Table 1S), we hypothesized that small molecule inhibitors that
437 interrupt gastrulation of zebrafish embryos might suppress metastatic progression of
438 human cancer cells. We created a unique screening concept utilizing gastrulation of
439 zebrafish embryos to test the hypothesis. Our results clearly confirmed our hypothesis:
440 25.6% (20/76 drugs) of epiboly-interrupting drugs could also suppress cell motility and
441 invasion of highly metastatic human cell lines in vitro. In particular, Pizotifen which is an
442 antagonist for serotonin receptor 2C and one of the epiboly-interrupting drugs, could
443 suppress metastasis in a mouse model (Figure 3A-E). Thus, this screen could offer a novel
444 platform for discovery of anti-metastasis drugs.
445 There are at least two advantages to the screen described herein. One is that the
446 screen can easily be converted to a chemical genetic screening platform. Indeed, we have
447 provided the first evidence that HTR2C, which is a primary target of Pizotifen, induced
448 EMT and promoted metastatic dissemination of cancer cells (Figure 4A-E). In this
449 research, 1,280 FDA approval drugs were screened, this is less than a few percent of all of
450 druggable targets (approximately 100 targets) in the human proteome in the body. If
451 chemical genetic screening using specific inhibitor libraries were conducted, more genes
452 that contribute to metastasis and gastrulation could be identified. The second advantage is
453 that the screen enables one researcher to test 100 drugs in 5 hours with using optical
454 microscopy, drugs, and zebrafish embryos. That indicates this screen is not only highly
455 efficient, low-cost, and low-labor but also enables researchers who do not have high
456 throughput screening instruments to conduct drug screening for anti-metastasis drugs.
457

458 **Acknowledgments**

459 We sincerely appreciate Dr. Joshua Collins (NIH/NIDCR) and Dr. Diane Palmieri
460 (NIH/NCI) for helping this research. We thank Dr. Herrick (Albany medical collage) for
461 providing pCMV-h5TH2C-VSV with us. This study was funded by grants from National

Medical Research Council of Singapore (R-154000547511) and Ministry of Education of Singapore (R-154000A23112) to Z.G.

Author Contributions

Design research; J.N. Conducting experiments; J.N. and L.T. Analyzing data: J.N. Writing the paper; J.N. and Z.G. Funding Acquisition; Z.G, S.W. B.C.G., H.M. and Supervision; Z.G.

Declaration of Interests

J.N., L.T., B.C.G., S.W., H.M. and G.Z. declare no conflict of interest.

Materials and Methods

Zebrafish embryo screening

Zebrafish embryos at two cell stage were collected at 20 mins after their fertilization. Each drug was added to a well of a 24-well plate containing approximately 20 zebrafish embryos per well in either 10 μM or 50 μM final concentration when the embryos reached the sphere stage. Chemical treatment was initiated at 4 hours post-fertilization (hpf) and approximately 20 embryos were treated with two different concentrations for each compound tested. The treatment was ended at 9 hpf when vehicle (DMSO) treated embryos as control reach 80-90% completion of the epiboly stage. The compounds which induced delay (<50% epiboly) in epiboly were selected as hit compounds for in vitro testing using highly metastatic human cancer cell lines. The study protocol was approved by the Institutional Animal Care and Use Committee of the National University of Singapore (protocol number: R16-1068).

Reagents

488 FDA, EMA and other agencies approved chemical libraries was purchased from
489 Prestwick Chemical (Illkirch, France). Pizotifen and S(-) Eticlopride hydrochloride were
490 purchased from Sigma-Aldrich (St. Louis, MO).
491
492 **Cell culture and cell viability assay**
493 MCF7, MDA-MB-231, MDA-MB-435, MIA-PaCa2, PC3, SW620, PC9 and HaCaT cells
494 were obtained from American Type Culture Collection (ATCC, Manassas, VA).
495 Luciferase-expressing 4T1 (4T1-12B) cells were provided from Dr. Gary Sahagian (Tufts
496 University, Boston, MA). All culture methods followed the supplier's instruction. Cell
497 viability assay was performed as previously described (16).
498
499 **Plasmid**
500 A DNA fragment coding for HTR2C was amplified by PCR with primers containing
501 restriction enzyme recognition sequences. The HTR2C coding fragment was amplified
502 from hsp70l:mCherry-T2A-CreERT2 plasmid (17).
503
504 **Immunoblotting**
505 Western blotting was performed as described previously (16). Anti-PRMT1, anti-
506 CYP11A1, anti-E-cadherin, anti-EpCAM, anti-Vimentin, anti-N-cadherin, anti-Zeb1,
507 anti-Histone H_3, anti-α-tubulin and anti-GAPDH antibodies were purchased from Cell
508 signaling Technology. Anti-HTR2C and anti-DRD2 antibodies were purchased form
509 Abcam. Anti-phospho-GSK3β (Ser9), anti-GSK3β, Anti-KRT18, anti-KRT19, anti-
510 MMP1, anti-MMP2, anti-S100A4, anti-Luciferase, and anti-β-catenin antibodies were
511 purchased from Santa Cruz.
512
513 **Flow cytometry**

514 Cells were stained with FITC-conjugated E-cadherin antibody (Biolegend, San Diego,
515 CA). Flow cytometry was performed as described (26) and analyzed with FlowJo
516 software (TreeStar, Ashland, OR).
517
518 **shRNA mediated gene knockdown**
519 The short hairpin RNA (shRNA)-expressing lentivirus vectors were
520 constructed using pLVX-shRNA1 vector (Clontech). PRMT1-shRNA_#3–targeting
521 sequence is GTGTTCCAGTATCTCTGATTA; PRMT1-shRNA_#4–targeting sequence
522 is TTGACTCCTACGCACACTTTG. CYP11A1-shRNA_#4–targeting sequence is
523 GCGATTCATTGATGCCATCTA; CYP11A1-shRNA_#4–targeting sequence is
524 GAAATCCAACACCTCAGCGAT. Human HTR2C-shRNA–targeting sequence is
525 TCATGCACCTCTGCGCTATAT. Mouse HTR2C-shRNA–targeting sequence is
526 CTTCATACCGCTGACGATTAT. LacZ-shRNA– targeting sequence is
527 CTACACAAATCAGCGATT.
528
529 **Immunofluorescence**
530 Immunofluorescence microscopy assay was performed by previously described (16). Goat
531 anti-mouse and goat anti-rabbit immunoglobulin G (IgG) antibodies conjugated to Alexa
532 Fluor 488 (Life Technologies) and diluted at 1:100 were used. Nuclei were visualized by
533 the addition of 2μg/ml of 4', 6-diamidino-2-phenylindole (DAPI) and photographed at
534 100x magnification by a fluorescent microscope BZ-X700 (KEYENCE, Japan).
535
536 **Boyden chamber cell motility and invasion assay**
537 These assays were performed by previously described (16). In Boyden chamber assay,
538 either $3x10^5$ MDA-MB-231, $1x10^6$ MDA-MB-435, or $5x10^5$ PC9 cells were applied to
539 each well in the upper chamber.
540

541 **Zebrafish xenotransplantation model**

542 *Tg(kdrl:eGFP)* zebrafish was provided by Dr. Stainier (Max Planck Institute for Heart and
543 Lung Research). Embryos that were derived from the line were maintained in E3 medium
544 containing 200μM 1-phenyl-2-thiourea (PTU). Approximately 100-400 Red fluorescence
545 protein (RFP)-labelled MBA-MB-231 or MIA-Paca2 cells were injected into the duct of
546 Cuvier of the zebrafish at 2dpf. The fish were randomly assigned to two groups. One group
547 was maintained in the presence of pizotifen-containing E3 medium and the other group was
548 maintained in vehicle-containing E3 medium.

549

550 **Spontaneous metastasis mouse model**

551 4T1-12B cells ($2x10^4$) were injected into the #4 mammary fat pad while the mice were
552 anesthetized. To monitor tumor growth and metastases, mice were imaged biweekly by
553 IVIS Imaging System (ParkinElmer). The primary tumor was resected 10 days after
554 inoculation. The study protocol (protocol number: BRC IACUC #110612) was approved
555 by A*STAR (Agency for Science, Technology and Research, Singapore).

556

557 **Histological Analysis**

558 All OCT embedded primary tumors, lungs, and livers of mice from the spontaneous
559 metastasis 4T1 model were sectioned on a cryostat. Eight micron sections were taken at
560 five hundred micron intervals through the entirety of the livers and lungs. Sections were
561 subsequently stained with hematoxylin and eosin. Metastatic lesions were counted under a
562 microscope in each section for both lungs and livers.

563

564 **Statistics**

565 Data were analyzed by Student's t test; $p < 0.05$ was considered significant.

566

567 **References**

568 1. Chambers AF, Groom AC, & MacDonald IC (2002) Dissemination and growth
569 of cancer cells in metastatic sites. *Nature reviews. Cancer* 2(8):563-572.
570 2. Steeg PS (2003) Metastasis suppressors alter the signal transduction of
571 cancer cells. *Nature reviews. Cancer* 3(1):55-63.
572 3. Fidler IJ (2003) The pathogenesis of cancer metastasis: the 'seed and soil'
573 hypothesis revisited. *Nature reviews. Cancer* 3(6):453-458.
574 4. Cavallaro U & Christofori G (2004) Cell adhesion and signalling by cadherins
575 and Ig-CAMs in cancer. *Nature reviews. Cancer* 4(2):118-132.
576 5. Ellenbroek SI, Iden S, & Collard JG (2012) Cell polarity proteins and cancer.
577 *Semin Cancer Biol* 22(3):208-215.
578 6. Tsai JH & Yang J (2013) Epithelial-mesenchymal plasticity in carcinoma
579 metastasis. *Genes & development* 27(20):2192-2206.
580 7. Solnica-Krezel L (2005) Conserved patterns of cell movements during
581 vertebrate gastrulation. *Curr Biol* 15(6):R213-228.
582 8. Latimer A & Jessen JR (2010) Extracellular matrix assembly and organization
583 during zebrafish gastrulation. *Matrix Biol* 29(2):89-96.
584 9. Solnica-Krezel L (2006) Gastrulation in zebrafish -- all just about adhesion?
585 *Curr Opin Genet Dev* 16(4):433-441.
586 10. Tsai YJ*, et al.* (2011) The predominant protein arginine methyltransferase
587 PRMT1 is critical for zebrafish convergence and extension during
588 gastrulation. *FEBS J* 278(6):905-917.
589 11. Hsu HJ, Liang MR, Chen CT, & Chung BC (2006) Pregnenolone stabilizes
590 microtubules and promotes zebrafish embryonic cell movement. *Nature*
591 439(7075):480-483.
592 12. Weinbach EC & Garbus J (1969) Mechanism of Action of Reagents that
593 uncouple Oxidative Phosphorylation. *Nature* 221:1016.
594 13. Sack U*, et al.* (2011) Novel effect of antihelminthic Niclosamide on S100A4-
595 mediated metastatic progression in colon cancer. *Journal of the National*
596 *Cancer Institute* 103(13):1018-1036.
597 14. Huang EW*, et al.* (2012) Vinpocetine inhibits breast cancer cells growth in
598 vitro and in vivo. *Apoptosis : an international journal on programmed cell*
599 *death* 17(10):1120-1130.
600 15. Szilágyi G*, et al.* (2005) Effects of vinpocetine on the redistribution of cerebral
601 blood flow and glucose metabolism in chronic ischemic stroke patients: a PET
602 study. *Journal of the Neurological Sciences* 229-230:275-284.
603 16. Nakayama J, Lu J, Makinoshima H, & Gong Z (2020) A Novel Zebrafish Model
604 of Metastasis Identifies the HSD11β1 Inhibitor Adrenosterone as a
605 Suppressor of Epithelial-Mesenchymal Transition and Metastatic
606 Dissemination. *Mol Cancer Res* 18(3):477-487.
607 17. Kolosionek E*, et al.* (2009) Expression and activity of phosphodiesterase
608 isoforms during epithelial mesenchymal transition: the role of
609 phosphodiesterase 4. *Mol Biol Cell* 20(22):4751-4765.
610 18. Sasaki T*, et al.* (2014) Serum CD10 is associated with liver metastasis in
611 colorectal cancer. *J Surg Res.* 192(2):390-394.
612 19. Liu P*, et al.* (2013) Disulfiram targets cancer stem-like cells and reverses
613 resistance and cross-resistance in acquired paclitaxel-resistant triple-
614 negative breast cancer cells. *British journal of cancer* 109(7):1876-1885.
615 20. Gunnarsson L, Jauhiainen A, Kristiansson E, Nerman O, & Larsson DGJ (2008)
616 Evolutionary conservation of human drug targets in organisms used for
617 environmental risk assessments. *Environmental Science & Technology*
618 42(15):5807-5813.
619 21. Tao K, Fang M, Alroy J, & Sahagian GG (2008) Imagable 4T1 model for the
620 study of late stage breast cancer. *BMC cancer* 8:228.

621 22. Kröger C, Afeyan, A.; Mraz, J.; Eaton, EN.; Reinhardt, F.; Khodor, YL.; Thiru, P.;
622 Bierie B.; Ye, X.; Burge, CB.; Weinberg RA (2019) Acquisition of a hybrid E/M
623 state is essential for tumorigenicity of basal breast cancer cells. *Proceedings*
624 *of the National Academy of Sciences of the United States of America*
625 116(15):7353-7362.
626 23. Beyer TD, M.; Thumberger, T.; Vick, P.; Tisler, M.; Schneider, I.; Bogusch, S.;
627 Andre, P.; Ulmer, B.; Walentek, P.; Niesler, B.; Blum, M.; Schweickert, A.
628 (2012) Serotonin signaling is required for Wnt-dependent GRP specification
629 and leftward flow in Xenopus. *Curr Biol* 22(1):33-39.
630 24. Sui HX, H.; Ji, Q.; Liu, X.; Zhou, L.; Song, H.; Zhou, X.; Xu, Y.; Chen, Z.; Cai, J.; Ji, G.;
631 Li, Q. (2015) 5-hydroxytryptamine receptor (5-HT1DR) promotes colorectal
632 cancer metastasis by regulating Axin1/β-catenin/MMP-7 signaling pathway.
633 *Oncotarget* 6(28):25975-25987.
634 25. Zhan TR, N.; Boutros, M. (2017) Wnt signaling in cancer. *Oncogene*
635 36(11):1461–1473.
636 26. Nakayama J*, et al.* (2009) BLNK suppresses pre-B-cell leukemogenesis
637 through inhibition of JAK3. *Blood* 113(7):1483-1492.
638

639

640 **Supplemental Information**

641

642 **Figure S1.**

643

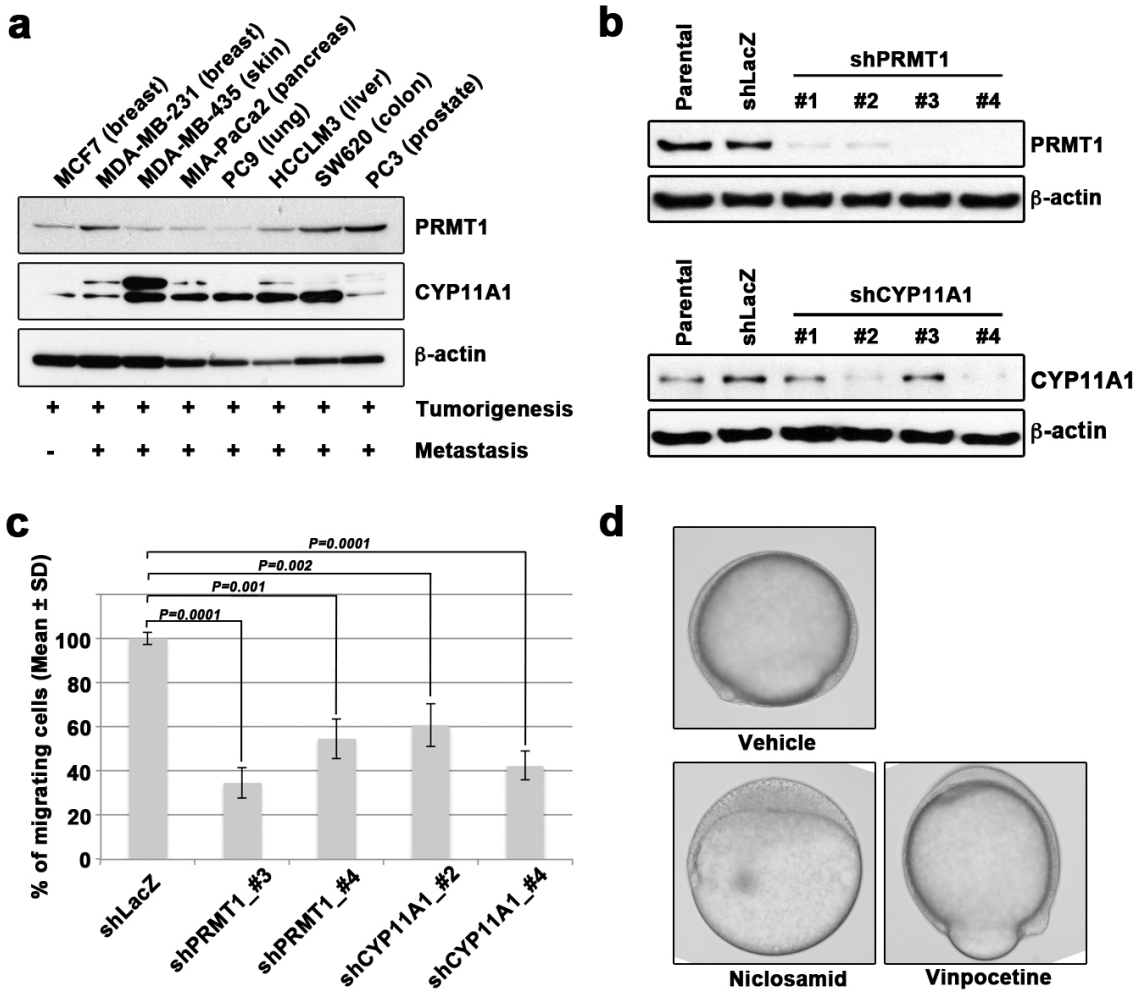

644

645

646 **Figure S1. Molecular mechanisms of epiboly in zebrafish overlap with those in**

647 **cancer metastasis.**

648 (A) Western blot analysis of PRMT1 (upper) and CYP11A1 (middle) protein levels in

649 non-metastatic human cancer cell line (MCF7) and highly metastatic human cancer cell

650 lines (MDA-MB-231, MDA-MB-435, MIA-PaCa2, PC9, HCCLM3, PC3 and SW620); β-

651 actin loading control is shown (bottom). (B) Knockdown of PRMT1 or CYP11A1 in

652 MDA-MB-231 cells. MBA-MB-231 cells were transfected with a control shRNA

653 targeting LacZ, and one of four independent shRNAs targeting PRMT1 (clone #1 to

654 #4) or one of two independent shRNAs targeting CYP11A1 (clone #1 to #4). Reduced

655 PRMT1 and CYP11A1 expression, determined by western blot, in sub-cell lines of

656 MDA-MB-231 cells expressing PRMT1 shRNA (clone #3 and #4 or CYP11A1 (clone
657 #2 and #4), compared with controls (parental cell line MDA-MB-231 and control
658 shRNA cells); β-actin levels shown as a loading control. (C) Effect of shRNAs
659 targeting either PRMT1 or CYP11A1 on cell motility and invasion of MBA-MB-231
660 cells. Parental MDA-MB-231 cells and four sub-cell lines of MDA-MB-231 cells that
661 were transfected with either shRNA targeting either LacZ, two independent shRNAs
662 targeting PRMT1 (clone #3 and #4) or two independent shRNAs targeting CYP11A1
663 (clone #2 and #4), were subjected to Boyden chamber assays. (D) Zebrafish embryos
664 treated with either vehicle (DMSO), 10μM Niclosamide, or 50μM vinpocetine.
665 Approximately 20 embryos were treated with either DMSO as a vehicle control,
666 niclosamide, or vinpocetine. The treatment was started at 4 hpf when all of embryos
667 reached sphere stage and ended at 9 hpf when control embryos reached 80-90%
668 epiboly stage. Each experiment was performed at least twice. Statistical analysis was
669 determined by Student's *t* test.
670

671
672 **Figure S2.**

673

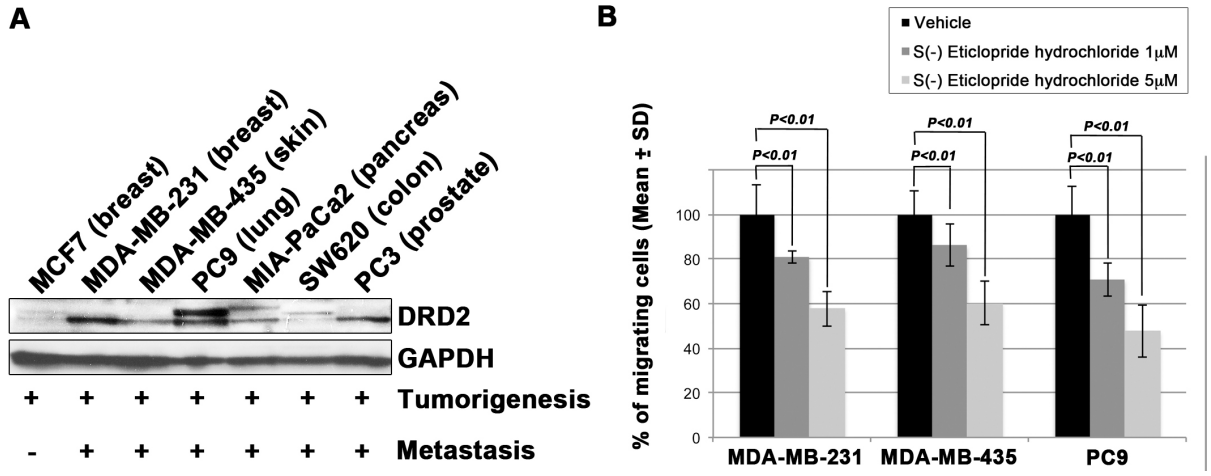

674

675

676 **Figure S2. S (-) Eticlopride hydrochloride suppressed cell motility and invasion of**

677 **human cancer cells.**

678 Related to Figure 2.

679 (A) Western blot analysis of DRD2 levels in non-metastatic human cancer cell line,

680 MCF7 (breast) and highly metastatic human cancer cell lines, MDA-MB-231 (breast),

681 MDA-MB-435 (melanoma), MIA-PaCa2 (pancreas), PC3 (prostate) and SW620 (colon);

682 GAPDH loading control is shown (bottom). (B) Effect of S (-) Eticlopride hydrochloride

683 on cell motility and invasion of MBA-MB-231, MDA-MB-435, and PC9 cells. Either

684 vehicle or pizotifen treated cells were subjected to Boyden chamber assays. Fetal bovine

685 serum (1%v/v) was used as the chemoattractant in both assays. Each experiment was

686 performed at least twice. Statistical analysis was determined by Student's *t* test.

687

688

689 **Figure S3.**

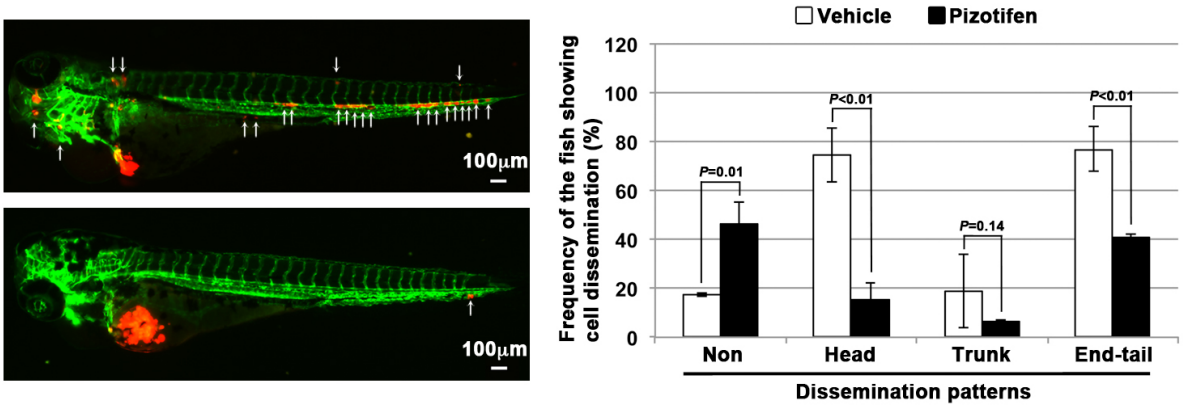

690

691 **Figure S3. Pizotifen suppressed metastatic dissemination of human pancreatic**

692 **cancer cells in a zebrafish xenotransplantation model.**

693 Related to Figure 2.

694 Representative images of dissemination of MIA-PaCa2 cells in zebrafish

695 xenotransplantation model. The fish were inoculated with MIA-PaCa2 cells, and treated

696 with either vehicle (top left) or drug (lower left). White arrows heads indicate

697 disseminated MIA-PaCa2 cells. The images were shown in 4x magnification. Scale bar,

698 100μm. The mean frequencies of the fish showing head, trunk, or end-tail dissemination

699 were tabulated (right). Each value is indicated as the mean ± SEM of two independent

700 experiments. Statistical analysis was determined by Student's *t* test.

701

702 **Table S1. A list of the genes that are involved between gastrulation and**
703 **metastasis progression**
704

Genes	Gastrulation Defects	Ref	Effects in Metastasis	Ref
BMP	Convergence and extension	(1)	EMT	(2)
WNT	Convergence and extension	(3)	Migration and Invasion	(4)
FGF	Convergence and extension	(5)	Invision	(6)
EGF	Epiboly	(7)	Migration	(8)
PDGF	Convergence and extension	(9)	EMT	(10)
CXCL12	Migration of endodermal cells	(11)	Migration and Invasion	(12)
CXCR4	Migration of endodermal cells	(11)	Migration and Invasion	(12)
PIK3CA	Convergence and extension	(13)	Migration and Invasion	(14)
YES	Epiboly	(15)	Migration	(16)
FYN	Epiboly	(17)	Migration and Invasion	(18)
MAPK1	Epiboly	(19)	Migration	(20)
SHP2	Convergence and extension	(21)	Migration	(22)
SNAI1	Convergence and extension	(23)	EMT	(24)
SNAI2	Mesoderm & Neural crest formation	(25)	EMT	(95)
TWIST1	Mesoderm formation	(26)	EMT	(27)
TBXT	Convergence and extension	(3)	EMT	(28)
ZEB1	Epiboly	(29)	EMT	(30)
GSC	Mesodermal patterning	(31)	EMT	(32)
FOXC2	Unclear, defects in gastrulation	(33)	EMT	(34)
STAT3	Convergence and extension	(35)	Migration	(36)
POU5F1	Epiboly	(37)	EMT	(38)
EZH2	Unclear, defects in gastrulation	(39)	Invasion	(40)
EHMT2	Defects in Neurogenesis	(41)	Migration and Invasion	(42)
BMI1	Defects in skelton formation	(43)	EMT	(44)
RHOA	Convergence and extension	(45)	Migration and Invasion	(46)
CDC42	Convergence and extension	(47)	Migration and Invasion	(48)
RAC1	Convergence and extension	(49)	Migration and Invasion	(50)
ROCK2	Convergence and extension	(51)	Migration and Invasion	(52)
PAR1	Convergence and extension	(53)	Migration	(54)
PRKCI	Convergence and extension	(53)	EMT	(55)
CAP1	Convergence and extension	(56)	Migration	(57)
EZR	Epiboly	(58)	Migration	(59)
EPCAM	Epiboly	(60)	Migration and Invasion	(61)
ITGB1 / ITA5	Mesodermal Migration	(62)	Migration and Invasion	(63)
FN1	Convergence and extension	(64)	Invasion	(65)
HAS2	Dorsal migration of lateral cells	(66)	Invasion	(67)
MMP14	Convergence and extension	(68)	Invasion	(69)
COX1	Epiboly	(70)	Invasion	(71)
PTGES	Convergence and extension	(72)	Invasion	(73)
SLC39A6	Aterior migration	(74)	EMT	(75)
GNA12 / 13	Convergence and extension	(41)	Migration and Invasion	(76)
OGT	Epiboly	(77)	Migration and Invasion	(78)
CCN1	Cell Movement	(79)	Migration and Invasion	(80)
TRPM7	Convergence and extension	(81)	Migration	(82)
MAPKAPK2	Epiboly	(83)	Migration	(84)
B4GALT1	Convergence and extension	(85)	Invasion	(86)
IER2	Convergence and extension	(87)	Migration	(88)
TIP1	Convergence and extension	(89)	Migration and Invasion	(90)
PAK5	Convergence and extension	(91)	Migration	(92)
MARCKS	Convergence and extension	(93)	Migration and Invasion	(94)

705

706 **Table S1.**

707 A list of the fifty genes that play essential role in governing both metastasis and

708 gastrulation progression. The gastrulation defects in Xenopus or zebrafish that are

709 induced by knockdown of each of these genes, were indicated. The molecular

710 mechanism in metastasis that are inhibited by knockdown of each of the same genes,

711 were indicated.

712 **Table S2. A list of the drugs that interfere with epiboly progression in zebrafish**
713

Chemical name	Chemical formula	Effect of 10uM	Effect of 50uM
Acitretin	C21H26O3	Delayed	Delayed
Adrenosterone	C19H24O3	Delayed	Delayed
Albendazole	C12H15N3O2S	Severe delayed	Severe delayed
Alfadolone acetate	C23H34O5	Delayed	Delayed
Alfaxalone	C21H32O3	Delayed	Delayed
Alprostadil	C20H34O5	Delayed	Delayed
Altrenogest	C21H26O2	Slightly delayed	Delayed
Ampiroxicam	C20H21N3O7S	Non effect	Delayed
Anethole-trithione	C10H8OS3	Delayed	Delayed
Antimycin A	C28H40N2O9	Delayed	Delayed
Avobenzone	C20H22O3	Delayed	Delayed
Benzoxiquine	C16H11NO2	Non effect	Delayed
Bosentan	C27H29N5O6S	Delayed	Delayed
Butoconazole nitrate	C19H18Cl3N3O3S	Delayed	Toxic lethal
Camptothecine (S,+)	C20H16N2O4	Severe delayed	Severe delayed
Carbenoxolone disodium salt	C34H48Na2O7	Delayed	Toxic lethal
Carmofur	C11H16FN3O3	Slightly delayed	Delayed
Carprofen	C15H12ClNO2	Severe delayed	Toxic lethal
Cefdinir	C14H13N5O5S2	Delayed	Delayed
Celecoxib	C17H14F3N3O2S	Delayed	Delayed
Chlorambucil	C14H19Cl2NO2	Slightly delayed	Delayed
Chlorhexidine	C22H30Cl2N10	Non effect	Toxic lethal
Ciclopirox ethanolamine	C14H24N2O3	Delayed	Severe delayed
Cinoxacin	C12H10N2O5	Delayed	Severe delayed
Clofibrate	C12H15ClO3	Non effect	Severe delayed
Clopidogrel	C16H16ClNO2S	Non effect	Delayed
Clorgyline hydrochloride	C13H16Cl3NO	Delayed	Delayed
Colchicine	C22H25NO6	Non effect	Delayed
Deptropine citrate	C29H35NO8	Delayed	Delayed
Desipramine hydrochloride	C18H23ClN2	Delayed	Delayed
Diclofenac sodium	C14H10Cl2NNaO2	Delayed	Severe delayed
Dicumarol	C19H12O6	Delayed	Severe delayed
Diethylstilbestrol	C18H20O2	Delayed	Toxic lethal
Dimaprit dihydrochloride	C6H17Cl2N3S	Slightly delayed	Delayed
Disulfiram	C10H20N2S4	Delayed	Delayed
Dopamine hydrochloride	C8H12ClNO2	Delayed	Delayed
Eburnamonine (-)	C19H22N2O	Delayed	Delayed
Ethaverine hydrochloride	C24H30ClNO4	Delayed	Delayed
Ethinylestradiol	C20H24O2	Delayed	Severe delayed
Ethopropazine hydrochloride	C19H25ClN2S	Delayed	Delayed
Ethoxyquin	C14H19NO	Non effect	Delayed
Exemestane	C20H24O2	Slightly delayed	Delayed
Ezetimibe	C24H21F2NO3	Slightly delayed	Delayed
Fenbendazole	C15H13N3O2S	Non effect	Delayed
Fenoprofen calcium salt dihydrate	C30H30CaO8	Slightly delayed	Delayed
Fentiazac	C17H12ClNO2S	Toxic lethal	Toxic lethal
Floxuridine	C9H11FN2O5	Delayed	Toxic lethal
Flunixin meglumine	C21H28F3N3O7	Delayed	Toxic lethal
Flutamide	C11H11F3N2O3	Delayed	Toxic lethal
Fluticasone propionate	C25H31F3O5S	Non effect	Delayed
Furosemide	C12H11ClN2O5S	Delayed	Delayed
Gatifloxacin	C19H22FN3O4	Delayed	Delayed
Gemcitabine	C9H11F2N3O4	Delayed	Delayed
Gemfibrozil	C15H22O3	Delayed	Toxic lethal
Gestrinone	C21H24O2	Delayed	Delayed
Haloprogin	C9H4Cl3IO	Delayed	Toxic lethal
Hexachlorophene	C13H6Cl6O2	Delayed	Severe delayed
Hexestrol	C18H22O2	Slightly delayed	Delayed
Ibudilast	C14H18N2O	Non effect	Delayed
Idazoxan hydrochloride	C11H13ClN2O2	Slightly delayed	Delayed
Idazoxan hydrochloride	C11H13ClN2O2	Non effect	Delayed

Idebenone	C19H30O5	Severe delayed	Toxic lethal
Indomethacin	C19H16ClNO4	Non effect	Delayed
Ipriflavone	C18H16O3	Delayed	Severe delayed
Isotretinoin	C20H28O2	Non effect	Severe delayed
Isradipine	C19H21N3O5	Non effect	Delayed
Lansoprazole	C16H14F3N3O2S	Slightly delayed	Delayed
Latanoprost	C26H40O5	Non effect	Delayed
Leflunomide	C12H9F3N2O2	Delayed	Severe delayed
Letrozole	C17H11N5	Non effect	Delayed
Lithocholic acid	C24H40O3	Non effect	Delayed
Lodoxamide	C11H6ClN3O6	Non effect	Delayed
Lofepramine	C26H27ClN2O	Non effect	Delayed
Loratadine	C22H23ClN2O2	Delayed	Delayed
Loxapine succinate	C22H24ClN3O5	Delayed	Delayed
Mebendazole	C16H13N3O3	Severe delayed	Severe delayed
Mebendazole	C22H26N2O2	Non effect	Delayed
Meloxicam	C14H13N3O4S2	Delayed	Toxic lethal
Methiazole	C12H15N3O2S	Delayed	Delayed
Mevastatin	C23H34O5	Non effect	Delayed
MK 801 hydrogen maleate	C20H19NO4	Slightly delayed	Delayed
Nabumetone	C15H16O2	Non effect	Severe delayed
Naftopidil dihydrochloride	C24H30Cl2N2O3	Slightly delayed	Delayed
Nandrolone	C18H26O2	Delayed	Delayed
Naproxen sodium salt	C14H13NaO3	Delayed	Delayed
Niclosamide	C13H8Cl2N2O4	Delayed	Delayed
Nifekalant	C19H27N5O5	Delayed	Delayed
Niflumic acid	C13H9F3N2O2	Delayed	Delayed
Nimesulide	C13H12N2O5S	Non effect	Delayed
Nisoldipine	C20H24N2O6	Delayed	Toxic lethal
Nitazoxanide	C12H9N3O5S	Severe delayed	Severe delayed
Norethindrone	C20H26O2	Non effect	Delayed
Norgestimate	C23H31NO3	Slightly delayed	Delayed
Oxfendazol	C15H13N3O3S	Slightly delayed	Delayed
Oxibendazol	C12H15N3O3	Severe delayed	Severe delayed
Oxymetholone	C21H32O3	Slightly delayed	Delayed
Parbendazole	C13H17N3O2	Severe delayed	Severe delayed
Parthenolide	C15H20O3	Non effect	Delayed
Penciclovir	C10H15N5O3	Non effect	Delayed
Pentobarbital	C11H18N2O3	Non effect	Delayed
Phenazopyridine hydrochloride	C11H12ClN5	Delayed	Toxic lethal
Phenothiazine	C12H9NS	Non effect	Delayed
Phenoxybenzamine hydrochloride	C18H23Cl2NO	Non effect	Delayed
Pizotifen malate	C23H27NO5S	Delayed	Severe delayed
Pramoxine hydrochloride	C17H28ClNO3	Slightly delayed	Delayed
Prilocaine hydrochloride	C13H21ClN2O	Non effect	Delayed
Primidone	C12H14N2O2	Slightly delayed	Delayed
Racecadotril	C21H23NO4S	Slightly delayed	Delayed
Riluzole hydrochloride	C8H6ClF3N2OS	Non effect	Delayed
Ritonavir	C37H48N6O5S2	Non effect	Severe delayed
S(-)Eticlopride hydrochloride	C17H26Cl2N2O3	Delayed	Delayed
Salmeterol	C25H37NO4	Non effect	Delayed
Streptomycin sulfate	C42H84N14O36S3	Non effect	Delayed
Sulconazole nitrate	C18H16Cl3N3O3S	Delayed	Delayed
Tegafur	C8H9FN2O3	Delayed	Delayed
Telmisartan	C33H30N4O2	Severe delayed	Toxic lethal
Tenatoprazole	C16H18N4O3S	Non effect	Delayed
Terbinafine	C21H25N	Non effect	Delayed
Thimerosal	C9H9HgNaO2S	Non effect	Delayed
Thiorphan	C12H15NO3S	Delayed	Delayed
Tolcapone	C14H11NO5	Severe delayed	Severe delayed
Topotecan	C23H23N3O5	Delayed	Delayed
Tracazolate hydrochloride	C16H25ClN4O2	Severe delayed	Delayed
Tribenoside	C29H34O6	Delayed	Delayed
Triclabendazole	C14H9Cl3N2OS	Delayed	Delayed
Triclosan	C12H7Cl3O2	Delayed	Severe delayed

Trioxsalen	C14H12O3	Delayed	Delayed
Troglitazone	C24H27NO5S	Severe delayed	Toxic lethal
Valproic acid	C8H16O2	Non effect	Delayed
Voriconazole	C16H14F3N5O	Non effect	Delayed
Zardaverine	C12H10F2N2O3	Slightly delayed	Delayed
Zuclopenthixol dihydrochloride	C22H27Cl3N2OS	Delayed	Delayed

714

715 **Table S2. A list of the drugs that interfere with epiboly progression in zebrafish.**

716 Related to Figure 1.

717 A list of positive "hit" drugs that interfered with epiboly progression. Gastrulation

718 defects or status of each of the zebrafish embryos that were treated with either 10μM

719 or 50μM concentrations, are indicated.

720

721 **Table S3. Effects of pharmacological inhibition of HTR2C on metastatic**
722 **dissemination of MDA-MB-231 cells in zebrafish xenografted models**
723

		Experiment _#1	Experiment _#2	Experiment _#3	Average of Experiments
Drug: Vehicle Cell: MDA-MB-231	Non-dissemination	0% n1=0/17	0% n2=0/12	6.66% n3=1/15	2.22±3.84%
	Head	58.82% n1=10/17	91.66% n2=11/12	6.66% n3=1/15	72.38±17.15%
	Trunk	52.94% n1=9/17	8.33% n2=1/12	20% n3=2/15	27.09±23.13%
	End-tail	100% n1=17/17	100% n2=12/12	86.66% n3=13/15	95.55±7.69%
Drug: Pizotifen Cell: MDA-MB-231	Non-dissemination	55% n1=11/20	31.57% n2=6/19	45.45 % n3=10/22	44.01±11.77%
	Head	5% n1=1/20	31.57% n2=6/19	18.18% n3=4/22	18.25±13.28%
	Trunk	5% n1=1/20	10.52% n2=2/19	4.45% n3=1/22	6.69±3.32%
	End-tail	45% n1=9/20	57.89% n2=11/19	50% n3=11/22	50.96±6.50%

724

725 Related to Figure 2D.

726 The numbers and frequencies of the fish showing the dissemination patterns in vehicle

727 or Pizotifen-treated group, were indicated. The fish showed both patterns of

728 dissemination were redundantly counted in this analysis.

729

730 **Table S4. Effects of pharmacological inhibition of HTR2C on metastatic**
731 **dissemination of Mia-PaCa2 cells in zebrafish xenografted models**
732

		Experiment _#1	Experiment _#2	Average of Experiments
Drug: Vehicle Cell: MIA-PaCa2	Non-dissemination	17.64% n1=3/17	16.66% n2=2/12	17.15+0.69%
	Head	82.35% n1=14/17	66.66% n2=8/12	74.50+11.09%
	Trunk	29.41% n1=5/17	8.33% n2=1/12	18.87+14.90%
	End-tail	70.58% n1=12/17	83.33% n2=10/17	76.96%+9.01
Drug: Pizotifen Cell: MIA-PaCa2	Non-dissemination	40% n1=4/10	52.63% n2=10/19	46.31+8.93%
	Head	20% n1=2/10	10.52% n2=2/19	15.26+6.69%
	Trunk	10% n1=1/10	5.26% n2=1/19	7.63+3.34%
	End-tail	40% n1=4/10	42.05% n2=8/19	41.4+1.48%

733
734
735 Related to Figure S3.

736 The numbers and frequencies of the fish showing the dissemination patterns in vehicle

737 or Pizotifen-treated group, were indicated. The fish showed both patterns of

738 dissemination were redundantly counted in this analysis.

739
740
741 **Table S5. Effects of genetic inhibition of HTR2C on metastatic dissemination of**
742 **MDA-MB-231 cells in zebrafish xenografted models**
743

		Experiment _#1	Experiment _#2	Average of Experiments
shLacZ	Non-dissemination	0% n1=0/10	0% n2=0/10	0%
	Head	60% n1=6/10	100% n2=10/10	80 ±28.28%
	Trunk	30% n1=3/10	10% n2=1/10	20±14.14%
	End-tail	80% n1=8/10	100% n2=10/10	90%±14.14
shHTR2C	Non-dissemination	80% n1=12/15	76.84% n2=14/19	76.84±4.46 %
	Head	6.66% n1=1/15	15.78% n2=3/19	11.22±6.45%
	Trunk	6.66% n1=1/15	5.26% n2=1/19	5.96±0.99%
	End-tail	20% n1=3/15	26.31% n2=5/19	23.15±4.46%

744
745 Related to Figure 2E.

746 The numbers and frequencies of the fish showing the dissemination patterns in the

747 zebrafish that were inoculated with either shLacZ or shHTR2C MDA-MB-231 cells,

748 were indicated. The fish showed both patterns of dissemination were redundantly

749 counted in this analysis.

750 **Table S6. Effects of HTR2C overexpression on metastatic dissemination of**
751 **MCF7 cells in zebrafish xenografted models**
752

		Experiment _#1	Experiment _#2	Average of Experiments
VC	Non-dissemination	46.15% n1=6/13	40% n2=4/10	43.07±4.35%
	Head	46.15% n1=6/13	20% n2=2/10	33.07±18.49%
	Trunk	0% n1=0/13	0% n2=0/10	0%
	End-tail	53.84% n1=7/13	60% n2=6/10	56.92±4.35
HTR2C	Non-dissemination	0% n1=0/14	0% n2=0/15	0%
	Head	100% n1=14/14	93.33% n2=14/15	96.66±4.71%
	Trunk	64.28% n1=9/14	73.33% n2=11/15	68.80±6.39%
	End-tail	85.71% n1=12/14	93.33% n2=14/15	89.52±5.38%

753

754 Related to Figure 4E.

755 The numbers and frequencies of the fish showing the dissemination patterns in the

756 zebrafish that were inoculated with MCF7 cells expressing either VC or HTR2C, were

757 indicated. The fish showed both patterns of dissemination were redundantly counted

758 in this analysis.

759
760
761 **References for Table S1.**

762 1. Kondo M (2007) Bone morphogenetic proteins in the early development
763 of zebrafish. *FEBS J* 274(12):2960-2967.
764 2. Katsuno Y, *et al.* (2008) Bone morphogenetic protein signaling enhances
765 invasion and bone metastasis of breast cancer cells through Smad
766 pathway. *Oncogene* 27(49):6322-6333.
767 3. Tada M & Smith JC (2000) Xwnt11 is a target of Xenopus Brachyury:
768 regulation of gastrulation movements via Dishevelled, but not through the
769 canonical Wnt pathway. *Development* 127:2227-2238.
770 4. Vincan E & Barker N (2008) The upstream components of the Wnt
771 signalling pathway in the dynamic EMT and MET associated with
772 colorectal cancer progression. *Clin Exp Metastasis* 25(6):657-663.
773 5. Yang X, Dormann D, Munsterberg AE, & Weijer CJ (2002) Cell movement
774 patterns during gastrulation in the chick are controlled by positive and
775 negative chemotaxis mediated by FGF4 and FGF8. *Dev Cell* 3(3):425-437.

776 6. Nomura S, *et al.* (2008) FGF10/FGFR2 signal induces cell migration and
777 invasion in pancreatic cancer. *Br J Cancer* 99(2):305-313.
778 7. Song S, *et al.* (2013) Pou5f1-dependent EGF expression controls E-
779 cadherin endocytosis, cell adhesion, and zebrafish epiboly movements.
780 *Dev Cell* 24(5):486-501.
781 8. Lu Z, Jiang G, Blume-Jensen P, & Hunter T (2001) Epidermal growth
782 factor-induced tumor cell invasion and metastasis initiated by
783 dephosphorylation and downregulation of focal adhesion kinase. *Mol Cell*
784 *Biol* 21(12):4016-4031.
785 9. Damm EW & Winklbauer R (2011) PDGF-A controls mesoderm cell
786 orientation and radial intercalation during Xenopus gastrulation.
787 *Development* 138(3):565-575.
788 10. Jechlinger M, *et al.* (2006) Autocrine PDGFR signaling promotes mammary
789 cancer metastasis. *J Clin Invest* 116(6):1561-1570.
790 11. Mizoguchi T, Verkade H, Heath JK, Kuroiwa A, & Kikuchi Y (2008)
791 Sdf1/Cxcr4 signaling controls the dorsal migration of endodermal cells
792 during zebrafish gastrulation. *Development* 135(15):2521-2529.
793 12. Shen HB, Gu ZQ, Jian K, & Qi J (2013) CXCR4-mediated Stat3 activation is
794 essential for CXCL12-induced cell invasion in bladder cancer. *Tumour Biol*
795 34(3):1839-1845.
796 13. Montero J-A, Kilian B, Chan J, Bayliss PE, & Heisenberg C-P (2003)
797 Phosphoinositide 3-Kinase Is Required for Process Outgrowth and Cell
798 Polarization of Gastrulating Mesendodermal Cells. *Current Biology*
799 13(15):1279-1289.
800 14. Wander SA, *et al.* (2013) PI3K/mTOR inhibition can impair tumor
801 invasion and metastasis in vivo despite a lack of antiproliferative action in
802 vitro: implications for targeted therapy. *Breast Cancer Res Treat*
803 138(2):369-381.
804 15. Tsai WB, Zhang X, Sharma D, Wu W, & Kinsey WH (2005) Role of Yes
805 kinase during early zebrafish development. *Dev Biol* 277(1):129-141.
806 16. Barraclough J, Hodgkinson C, Hogg A, Dive C, & Welman A (2007)
807 Increases in c-Yes Expression Level and Activity Promote Motility But Not
808 Proliferation of Human Colorectal Carcinoma Cells. *Neoplasia* 9(9):745-
809 IN732.
810 17. Sharma D, Holets L, Zhang X, & Kinsey WH (2005) Role of Fyn kinase in
811 signaling associated with epiboly during zebrafish development. *Dev Biol*
812 285(2):462-476.
813 18. Yadav V & Denning MF (2011) Fyn is induced by Ras/PI3K/Akt signaling
814 and is required for enhanced invasion/migration. *Mol Carcinog* 50(5):346-
815 352.
816 19. Krens SF, *et al.* (2008) Distinct functions for ERK1 and ERK2 in cell
817 migration processes during zebrafish gastrulation. *Dev Biol* 319(2):370-
818 383.
819 20. Radtke S, Milanovic M, & Rossé C (2013) ERK2 but not ERK1 mediates
820 HGF-induced motility in non-small cell lung carcinoma cell lines. *J Cell Sci.*
821 126(Pt11):2381-2391.
822 21. Jopling C, van Geemen D, & den Hertog J (2007) Shp2 knockdown and
823 Noonan/LEOPARD mutant Shp2-induced gastrulation defects. *PLoS Genet*
824 3(12):e225.
825 22. Wang FM, *et al.* (2005) SHP-2 promoting migration and metastasis of
826 MCF-7 with loss of E-cadherin, dephosphorylation of FAK and secretion of

827 MMP-9 induced by IL-1beta in vivo and in vitro. *Breast Cancer Res Treat*
828 89(1):5-14.
829 23. Ip YT & Gridley T (2002) Cell movements during gastrulation: snail
830 dependent and independent pathways. *Curr Opin Genet Dev* 12(4):423-
831 429.
832 24. Batlle E, Sancho E, Francí C, Domínguez D, & Monfar M (2000) The
833 transcription factor snail is a repressor of E-cadherin gene expression in
834 epithelial tumour cells. *Nat Cell Biol* 2(2):84-89.
835 25. Shi J, Severson C, Yang J, Wedlich D, & Klymkowsky MW (2011) Snail2
836 controls mesodermal BMP/Wnt induction of neural crest. *Development*
837 138(15):3135-3145.
838 26. Castanon I & Baylies MK (2002) A Twist in fate: evolutionary comparison
839 of Twist structure and function. *Gene* 287(1-2):11-22.
840 27. Yang J, *et al.* (2004) Twist, a master regulator of morphogenesis, plays an
841 essential role in tumor metastasis. *Cell* 117(7):927-939.
842 28. Fernando RI, *et al.* (2010) The T-box transcription factor Brachyury
843 promotes epithelial-mesenchymal transition in human tumor cells. *J Clin*
844 *Invest* 120(2):533-544.
845 29. Vannier C, Mock K, Brabletz T, & Driever W (2013) Zeb1 regulates E-
846 cadherin and Epcam (epithelial cell adhesion molecule) expression to
847 control cell behavior in early zebrafish development. *J Biol Chem*
848 288(26):18643-18659.
849 30. Spaderna S, *et al.* (2008) The transcriptional repressor ZEB1 promotes
850 metastasis and loss of cell polarity in cancer. *Cancer Res* 68(2):537-544.
851 31. Sander V, Reversade B, & De Robertis EM (2007) The opposing homeobox
852 genes Goosecoid and Vent1/2 self-regulate Xenopus patterning. *EMBO J*
853 26(12):2955-2965.
854 32. Hartwell KA, *et al.* (2006) The Spemann organizer gene, Goosecoid,
855 promotes tumor metastasis. *Proc Natl Acad Sci U S A* 103(50):18969-
856 18974.
857 33. Wilm B, James RG, Schultheiss TM, & Hogan BL (2004) The forkhead
858 genes, Foxc1 and Foxc2, regulate paraxial versus intermediate mesoderm
859 cell fate. *Dev Biol* 271(1):176-189.
860 34. Mani SA, *et al.* (2007) Mesenchyme Forkhead 1 (FOXC2) plays a key role
861 in metastasis and is associated with aggressive basal-like breast cancers.
862 *Proc Natl Acad Sci U S A* 104(24):10069-10074.
863 35. Miyagi C, *et al.* (2004) STAT3 noncell-autonomously controls planar cell
864 polarity during zebrafish convergence and extension. *J Cell Biol*
865 166(7):975-981.
866 36. Abdulghani J, *et al.* (2008) Stat3 promotes metastatic progression of
867 prostate cancer. *Am J Pathol* 172(6):1717-1728.
868 37. Lachnit M, Kur E, & Driever W (2008) Alterations of the cytoskeleton in all
869 three embryonic lineages contribute to the epiboly defect of Pou5f1/Oct4
870 deficient MZspg zebrafish embryos. *Dev Biol* 315(1):1-17.
871 38. Dai X, *et al.* (2013) OCT4 regulates epithelial-mesenchymal transition and
872 its knockdown inhibits colorectal cancer cell migration and invasion.
873 *Oncol Rep* 29(1):155-160.
874 39. O'Carroll D, *et al.* (2001) The polycomb-group gene Ezh2 is required for
875 early mouse development. *Mol Cell Biol* 21(13):4330-4336.

876 40. Ren G, *et al.* (2012) Polycomb protein EZH2 regulates tumor invasion via
877 the transcriptional repression of the metastasis suppressor RKIP in breast
878 and prostate cancer. *Cancer Res* 72(12):3091-3104.
879 41. Lin F, *et al.* (2005) Essential roles of G{alpha}12/13 signaling in distinct
880 cell behaviors driving zebrafish convergence and extension gastrulation
881 movements. *J Cell Biol* 169(5):777-787.
882 42. Chen MW, *et al.* (2010) H3K9 histone methyltransferase G9a promotes
883 lung cancer invasion and metastasis by silencing the cell adhesion
884 molecule Ep-CAM. *Cancer Res* 70(20):7830-7840.
885 43. van der Lugt NM, *et al.* (1994) Posterior transformation, neurological
886 abnormalities, and severe hematopoietic defects in mice with a targeted
887 deletion of the bmi-1 proto-oncogene. *Genes Dev* 8(7):757-769.
888 44. Guo BH, *et al.* (2011) Bmi-1 promotes invasion and metastasis, and its
889 elevated expression is correlated with an advanced stage of breast cancer.
890 *Mol Cancer* 10(1):10.
891 45. Zhu S, Liu L, Korzh V, Gong Z, & Low BC (2006) RhoA acts downstream of
892 Wnt5 and Wnt11 to regulate convergence and extension movements by
893 involving effectors Rho kinase and Diaphanous: use of zebrafish as an in
894 vivo model for GTPase signaling. *Cell Signal* 18(3):359-372.
895 46. Yoshioka K, Nakamori S, & Itoh K (1999) Overexpression of small GTP-
896 binding protein RhoA promotes invasion of tumor cells. *Cancer Res*
897 59(8):2004-2010.
898 47. Choi SC & Han JK (2002) Xenopus Cdc42 regulates convergent extension
899 movements during gastrulation through Wnt/Ca2+ signaling pathway.
900 *Dev Biol* 244(2):342-357.
901 48. Reymond N, *et al.* (2012) Cdc42 promotes transendothelial migration of
902 cancer cells through beta1 integrin. *J Cell Biol* 199(4):653-668.
903 49. Habas R, Dawid IB, & He X (2003) Coactivation of Rac and Rho by
904 Wnt/Frizzled signaling is required for vertebrate gastrulation. . *Genes Dev*
905 17(2):295-309.
906 50. Vega FM & Ridley AJ (2008) Rho GTPases in cancer cell biology. *FEBS Lett*
907 582(14):2093-2101.
908 51. Marlow F, Topczewski J, Sepich D, & Solnica-Krezel L (2002) Zebrafish
909 Rho kinase 2 acts downstream of Wnt11 to mediate cell polarity and
910 effective convergence and extension movements. *Curr Biol* 12(11):876-
911 884.
912 52. Itoh K, *et al.* (1999) An essential part for Rho-associated kinase in the
913 transcellular invasion of tumor cells. *Nat Med* 5(2):221-225.
914 53. Kusakabe M & Nishida E (2004) The polarity-inducing kinase Par-1
915 controls Xenopus gastrulation in cooperation with 14-3-3 and aPKC.
916 *EMBO J* 23(21):4190-4201.
917 54. Shi X, Gangadharan B, Brass LF, Ruf W, & Mueller BM (2004) Protease-
918 activated receptors (PAR1 and PAR2) contribute to tumor cell motility
919 and metastasis. *Mol Cancer Res* 2(7):395-402.
920 55. Gunaratne A, Thai BL, & Di Guglielmo GM (2013) Atypical protein kinase C
921 phosphorylates Par6 and facilitates transforming growth factor beta-
922 induced epithelial-to-mesenchymal transition. *Mol Cell Biol* 33(5):874-
923 886.
924 56. Seifert K, Ibrahim H, Stodtmeister T, Winklbauer R, & Niessen CM (2009)
925 An adhesion-independent, aPKC-dependent function for cadherins in
926 morphogenetic movements. *J Cell Sci* 122(Pt 14):2514-2523.

927 57. Yamazaki K, *et al.* (2009) Adenylate cyclase-associated protein 1
928 overexpressed in pancreatic cancers is involved in cancer cell motility.
929 *Lab Invest* 89(4):425-432.
930 58. Link V, *et al.* (2006) Identification of regulators of germ layer
931 morphogenesis using proteomics in zebrafish. *J Cell Sci* 119(Pt 10):2073-
932 2083.
933 59. Khanna C, *et al.* (2004) The membrane-cytoskeleton linker ezrin is
934 necessary for osteosarcoma metastasis. *Nat Med* 10(2):182-186.
935 60. Slanchev K, *et al.* (2009) The epithelial cell adhesion molecule EpCAM is
936 required for epithelial morphogenesis and integrity during zebrafish
937 epiboly and skin development. *PLoS Genet* 5(7):e1000563.
938 61. Ni J, *et al.* (2012) Role of the EpCAM (CD326) in prostate cancer
939 metastasis and progression. *Cancer Metastasis Rev* 31(3-4):779-791.
940 62. Skalski M, Alfandari D, & Darribere T (1998) A key function for alphav
941 containing integrins in mesodermal cell migration during Pleurodeles
942 waltl gastrulation. *Dev Biol* 195(2):158-173.
943 63. Felding-Habermann B (2003) Integrin adhesion receptors in tumor
944 metastasis. *Clin Exp Metastasis* 20(3):203-213.
945 64. Marsden M & DeSimone DW (2003) Integrin-ECM Interactions Regulate
946 Cadherin-Dependent Cell Adhesion and Are Required for Convergent
947 Extension in Xenopus. *Current Biology* 13(14):1182-1191.
948 65. Malik G, *et al.* (2010) Plasma fibronectin promotes lung metastasis by
949 contributions to fibrin clots and tumor cell invasion. *Cancer Res*
950 70(11):4327-4334.
951 66. Bakkers J, *et al.* (2004) Has2 is required upstream of Rac1 to govern
952 dorsal migration of lateral cells during zebrafish gastrulation.
953 *Development* 131(3):525-537.
954 67. Kim HR, *et al.* (2004) Hyaluronan facilitates invasion of colon carcinoma
955 cells in vitro via interaction with CD44. *Cancer Res* 64(13):4569-4576.
956 68. Coyle RC, Latimer A, & Jessen JR (2008) Membrane-type 1 matrix
957 metalloproteinase regulates cell migration during zebrafish gastrulation:
958 evidence for an interaction with non-canonical Wnt signaling. *Exp Cell Res*
959 314(10):2150-2162.
960 69. Perentes JY, *et al.* (2011) Cancer cell-associated MT1-MMP promotes
961 blood vessel invasion and distant metastasis in triple-negative mammary
962 tumors. *Cancer Res* 71(13):4527-4538.
963 70. Cha YI, *et al.* (2006) Cyclooxygenase-1-derived PGE2 promotes cell
964 motility via the G-protein-coupled EP4 receptor during vertebrate
965 gastrulation. *Genes Dev* 20(1):77-86.
966 71. Kundu N & Fulton AM (2002) Selective cyclooxygenase (COX)-1 or COX-2
967 inhibitors control metastatic disease in a murine model of breast cancer.
968 *Cancer Res* 62(8):2343-2346.
969 72. Speirs CK, *et al.* (2010) Prostaglandin Gbetagamma signaling stimulates
970 gastrulation movements by limiting cell adhesion through Snai1a
971 stabilization. *Development* 137(8):1327-1337.
972 73. Wang D & Dubois RN (2006) Prostaglandins and cancer. *Gut* 55(1):115-
973 122.
974 74. Yamashita S, *et al.* (2004) Zinc transporter LIVI controls epithelial-
975 mesenchymal transition in zebrafish gastrula organizer. *Nature*
976 429(6989):298-302.

977 75. Lue HW, *et al.* (2011) LIV-1 promotes prostate cancer epithelial-to-
978 mesenchymal transition and metastasis through HB-EGF shedding and
979 EGFR-mediated ERK signaling. *PLoS One* 6(11):e27720.
980 76. Yagi H, *et al.* (2011) A synthetic biology approach reveals a CXCR4-G13-
981 Rho signaling axis driving transendothelial migration of metastatic breast
982 cancer cells. *Sci Signal* 4(191):ra60.
983 77. Webster DM, *et al.* (2009) O-GlcNAc modifications regulate cell survival
984 and epiboly during zebrafish development. *BMC Dev Biol* 9:28.
985 78. Lynch TP, *et al.* (2012) Critical role of O-Linked beta-N-acetylglucosamine
986 transferase in prostate cancer invasion, angiogenesis, and metastasis. *J*
987 *Biol Chem* 287(14):11070-11081.
988 79. Latinkic BV (2003) Xenopus Cyr61 regulates gastrulation movements and
989 modulates Wnt signalling. *Development* 130(11):2429-2441.
990 80. Lin J, *et al.* (2012) A novel anti-Cyr61 antibody inhibits breast cancer
991 growth and metastasis in vivo. *Cancer Immunol Immunother* 61(5):677-
992 687.
993 81. Liu W, *et al.* (2011) TRPM7 regulates gastrulation during vertebrate
994 embryogenesis. *Dev Biol* 350(2):348-357.
995 82. Middelbeek J, *et al.* (2012) TRPM7 is required for breast tumor cell
996 metastasis. *Cancer Res* 72(16):4250-4261.
997 83. Holloway BA, *et al.* (2009) A novel role for MAPKAPK2 in morphogenesis
998 during zebrafish development. *PLoS Genet* 5(3):e1000413.
999 84. Kumar B, *et al.* (2010) p38 mitogen-activated protein kinase-driven
1000 MAPKAPK2 regulates invasion of bladder cancer by modulation of MMP-2
1001 and MMP-9 activity. *Cancer Res* 70(2):832-841.
1002 85. Machingo QJ, Fritz A, & Shur BD (2006) A beta1,4-galactosyltransferase is
1003 required for convergent extension movements in zebrafish. *Dev Biol*
1004 297(2):471-482.
1005 86. Zhu X, *et al.* (2005) Elevated beta1,4-galactosyltransferase I in highly
1006 metastatic human lung cancer cells. Identification of E1AF as important
1007 transcription activator. *J Biol Chem* 280(13):12503-12516.
1008 87. Hong SK, Tanegashima K, & Dawid IB (2011) XIer2 is required for
1009 convergent extension movements during Xenopus development. *Int J Dev*
1010 *Biol* 55(10-12):917-921.
1011 88. Neeb A, *et al.* (2012) The immediate early gene Ier2 promotes tumor cell
1012 motility and metastasis, and predicts poor survival of colorectal cancer
1013 patients. *Oncogene* 31(33):3796-3806.
1014 89. Besser J, Leito JT, van der Meer DL, & Bagowski CP (2007) Tip-1 induces
1015 filopodia growth and is important for gastrulation movements during
1016 zebrafish development. *Dev Growth Differ* 49(3):205-214.
1017 90. Han M, Wang H, Zhang HT, & Han Z (2012) The PDZ protein TIP-1
1018 facilitates cell migration and pulmonary metastasis of human invasive
1019 breast cancer cells in athymic mice. *Biochem Biophys Res Commun*
1020 422(1):139-145.
1021 91. Faure S, *et al.* (2005) Xenopus p21-activated kinase 5 regulates
1022 blastomeres' adhesive properties during convergent extension
1023 movements. *Dev Biol* 277(2):472-492.
1024 92. Gong W, *et al.* (2009) P21-activated kinase 5 is overexpressed during
1025 colorectal cancer progression and regulates colorectal carcinoma cell
1026 adhesion and migration. *Int J Cancer* 125(3):548-555.

1027 93. Iioka H, Ueno N, & Kinoshita N (2004) Essential role of MARCKS in cortical
1028 actin dynamics during gastrulation movements. *J Cell Biol* 164(2):169-
1029 174.
1030 94. Rombouts K, *et al.* (2013) Myristoylated Alanine-Rich protein Kinase C
1031 Substrate (MARCKS) expression modulates the metastatic phenotype in
1032 human and murine colon carcinoma in vitro and in vivo. *Cancer Lett*
1033 333(2):244-252.
1034
1035

1036 **Table S2. A list of the drugs that interfere with epiboly progression in zebrafish**
1037

Chemical name	Chemical formula	Effect of 10uM	Effect of 50uM
Acitretin	C21H26O3	Delayed	Delayed
Adrenosterone	C19H24O3	Delayed	Delayed
Albendazole	C12H15N3O2S	Severe delayed	Severe delayed
Alfadolone acetate	C23H34O5	Delayed	Delayed
Alfaxalone	C21H32O3	Delayed	Delayed
Alprostadil	C20H34O5	Delayed	Delayed
Altrenogest	C21H26O2	Slightly delayed	Delayed
Ampiroxicam	C20H21N3O7S	Non effect	Delayed
Anethole-trithione	C10H8OS3	Delayed	Delayed
Antimycin A	C28H40N2O9	Delayed	Delayed
Avobenzone	C20H22O3	Delayed	Delayed
Benzoxiquine	C16H11NO2	Non effect	Delayed
Bosentan	C27H29N5O6S	Delayed	Delayed
Butoconazole nitrate	C19H18Cl3N3O3S	Delayed	Toxic lethal
Camptothecine (S,+)	C20H16N2O4	Severe delayed	Severe delayed
Carbenoxolone disodium salt	C34H48Na2O7	Delayed	Toxic lethal
Carmofur	C11H16FN3O3	Slightly delayed	Delayed
Carprofen	C15H12ClNO2	Severe delayed	Toxic lethal
Cefdinir	C14H13N5O5S2	Delayed	Delayed
Celecoxib	C17H14F3N3O2S	Delayed	Delayed
Chlorambucil	C14H19Cl2NO2	Slightly delayed	Delayed
Chlorhexidine	C22H30Cl2N10	Non effect	Toxic lethal
Ciclopirox ethanolamine	C14H24N2O3	Delayed	Severe delayed
Cinoxacin	C12H10N2O5	Delayed	Severe delayed
Clofibrate	C12H15ClO3	Non effect	Severe delayed
Clopidogrel	C16H16ClNO2S	Non effect	Delayed
Clorgyline hydrochloride	C13H16Cl3NO	Delayed	Delayed
Colchicine	C22H25NO6	Non effect	Delayed
Deptropine citrate	C29H35NO8	Delayed	Delayed
Desipramine hydrochloride	C18H23ClN2	Delayed	Delayed
Diclofenac sodium	C14H10Cl2NNaO2	Delayed	Severe delayed
Dicumarol	C19H12O6	Delayed	Severe delayed
Diethylstilbestrol	C18H20O2	Delayed	Toxic lethal
Dimaprit dihydrochloride	C6H17Cl2N3S	Slightly delayed	Delayed
Disulfiram	C10H20N2S4	Delayed	Delayed
Dopamine hydrochloride	C8H12ClNO2	Delayed	Delayed
Eburnamonine (-)	C19H22N2O	Delayed	Delayed
Ethaverine hydrochloride	C24H30ClNO4	Delayed	Delayed
Ethinylestradiol	C20H24O2	Delayed	Severe delayed
Ethopropazine hydrochloride	C19H25ClN2S	Delayed	Delayed
Ethoxyquin	C14H19NO	Non effect	Delayed
Exemestane	C20H24O2	Slightly delayed	Delayed
Ezetimibe	C24H21F2NO3	Slightly delayed	Delayed
Fenbendazole	C15H13N3O2S	Non effect	Delayed
Fenoprofen calcium salt dihydrate	C30H30CaO8	Slightly delayed	Delayed
Fentiazac	C17H12ClNO2S	Toxic lethal	Toxic lethal
Floxuridine	C9H11FN2O5	Delayed	Toxic lethal
Flunixin meglumine	C21H28F3N3O7	Delayed	Toxic lethal
Flutamide	C11H11F3N2O3	Delayed	Toxic lethal
Fluticasone propionate	C25H31F3O5S	Non effect	Delayed
Furosemide	C12H11ClN2O5S	Delayed	Delayed
Gatifloxacin	C19H22FN3O4	Delayed	Delayed
Gemcitabine	C9H11F2N3O4	Delayed	Delayed
Gemfibrozil	C15H22O3	Delayed	Toxic lethal
Gestrinone	C21H24O2	Delayed	Delayed
Haloprogin	C9H4Cl3IO	Delayed	Toxic lethal
Hexachlorophene	C13H6Cl6O2	Delayed	Severe delayed
Hexestrol	C18H22O2	Slightly delayed	Delayed
Ibudilast	C14H18N2O	Non effect	Delayed
Idazoxan hydrochloride	C11H13ClN2O2	Slightly delayed	Delayed
Idazoxan hydrochloride	C11H13ClN2O2	Non effect	Delayed
Idebenone	C19H30O5	Severe delayed	Toxic lethal

Indomethacin	C19H16ClNO4	Non effect	Delayed
Ipriflavone	C18H16O3	Delayed	Severe delayed
Isotretinoin	C20H28O2	Non effect	Severe delayed
Isradipine	C19H21N3O5	Non effect	Delayed
Lansoprazole	C16H14F3N3O2S	Slightly delayed	Delayed
Latanoprost	C26H40O5	Non effect	Delayed
Leflunomide	C12H9F3N2O2	Delayed	Severe delayed
Letrozole	C17H11N5	Non effect	Delayed
Lithocholic acid	C24H40O3	Non effect	Delayed
Lodoxamide	C11H6ClN3O6	Non effect	Delayed
Lofepramine	C26H27ClN2O	Non effect	Delayed
Loratadine	C22H23ClN2O2	Delayed	Delayed
Loxapine succinate	C22H24ClN3O5	Delayed	Delayed
Mebendazole	C16H13N3O3	Severe delayed	Severe delayed
Mebendazole	C22H26N2O2	Non effect	Delayed
Meloxicam	C14H13N3O4S2	Delayed	Toxic lethal
Methiazole	C12H15N3O2S	Delayed	Delayed
Mevastatin	C23H34O5	Non effect	Delayed
MK 801 hydrogen maleate	C20H19NO4	Slightly delayed	Delayed
Nabumetone	C15H16O2	Non effect	Severe delayed
Naftopidil dihydrochloride	C24H30Cl2N2O3	Slightly delayed	Delayed
Nandrolone	C18H26O2	Delayed	Delayed
Naproxen sodium salt	C14H13NaO3	Delayed	Delayed
Niclosamide	C13H8Cl2N2O4	Delayed	Delayed
Nifekalant	C19H27N5O5	Delayed	Delayed
Niflumic acid	C13H9F3N2O2	Delayed	Delayed
Nimesulide	C13H12N2O5S	Non effect	Delayed
Nisoldipine	C20H24N2O6	Delayed	Toxic lethal
Nitazoxanide	C12H9N3O5S	Severe delayed	Severe delayed
Norethindrone	C20H26O2	Non effect	Delayed
Norgestimate	C23H31NO3	Slightly delayed	Delayed
Oxfendazol	C15H13N3O3S	Slightly delayed	Delayed
Oxibendazol	C12H15N3O3	Severe delayed	Severe delayed
Oxymetholone	C21H32O3	Slightly delayed	Delayed
Parbendazole	C13H17N3O2	Severe delayed	Severe delayed
Parthenolide	C15H20O3	Non effect	Delayed
Penciclovir	C10H15N5O3	Non effect	Delayed
Pentobarbital	C11H18N2O3	Non effect	Delayed
Phenazopyridine hydrochloride	C11H12ClN5	Delayed	Toxic lethal
Phenothiazine	C12H9NS	Non effect	Delayed
Phenoxybenzamine hydrochloride	C18H23Cl2NO	Non effect	Delayed
Pizotifen malate	C23H27NO5S	Delayed	Severe delayed
Pramoxine hydrochloride	C17H28ClNO3	Slightly delayed	Delayed
Prilocaine hydrochloride	C13H21ClN2O	Non effect	Delayed
Primidone	C12H14N2O2	Slightly delayed	Delayed
Racecadotril	C21H23NO4S	Slightly delayed	Delayed
Riluzole hydrochloride	C8H6ClF3N2OS	Non effect	Delayed
Ritonavir	C37H48N6O5S2	Non effect	Severe delayed
S(-)Eticlopride hydrochloride	C17H26Cl2N2O3	Delayed	Delayed
Salmeterol	C25H37NO4	Non effect	Delayed
Streptomycin sulfate	C42H84N14O36S3	Non effect	Delayed
Sulconazole nitrate	C18H16Cl3N3O3S	Delayed	Delayed
Tegafur	C8H9FN2O3	Delayed	Delayed
Telmisartan	C33H30N4O2	Severe delayed	Toxic lethal
Tenatoprazole	C16H18N4O3S	Non effect	Delayed
Terbinafine	C21H25N	Non effect	Delayed
Thimerosal	C9H9HgNaO2S	Non effect	Delayed
Thiorphan	C12H15NO3S	Delayed	Delayed
Tolcapone	C14H11NO5	Severe delayed	Severe delayed
Topotecan	C23H23N3O5	Delayed	Delayed
Tracazolate hydrochloride	C16H25ClN4O2	Severe delayed	Delayed
Tribenoside	C29H34O6	Delayed	Delayed
Triclabendazole	C14H9Cl3N2OS	Delayed	Delayed
Triclosan	C12H7Cl3O2	Delayed	Severe delayed
Trioxsalen	C14H12O3	Delayed	Delayed

Troglitazone	C24H27NO5S	Severe delayed	Toxic lethal
Valproic acid	C8H16O2	Non effect	Delayed
Voriconazole	C16H14F3N5O	Non effect	Delayed
Zardaverine	C12H10F2N2O3	Slightly delayed	Delayed
Zuclopenthixol dihydrochloride	C22H27Cl3N2OS	Delayed	Delayed

1038

1039 **Table S2. A list of the drugs that interfere with epiboly progression in zebrafish.**

1040 A list of positive "hit" drugs that interfered with epiboly progression. Gastrulation defects

1041 or status of each of the zebrafish embryos that were treated with either 10μM or 50μM

1042 concentrations, are indicated.

1043

1044

1045 **References for Table S1.**

1046 1. Kondo M (2007) Bone morphogenetic proteins in the early development of
1047 zebrafish. *FEBS J* 274(12):2960-2967.
1048 2. Katsuno Y, *et al.* (2008) Bone morphogenetic protein signaling enhances
1049 invasion and bone metastasis of breast cancer cells through Smad pathway.
1050 *Oncogene* 27(49):6322-6333.
1051 3. Tada M & Smith JC (2000) Xwnt11 is a target of Xenopus Brachyury:
1052 regulation of gastrulation movements via Dishevelled, but not through the
1053 canonical Wnt pathway. *Development* 127:2227-2238.
1054 4. Vincan E & Barker N (2008) The upstream components of the Wnt signalling
1055 pathway in the dynamic EMT and MET associated with colorectal cancer
1056 progression. *Clin Exp Metastasis* 25(6):657-663.
1057 5. Yang X, Dormann D, Munsterberg AE, & Weijer CJ (2002) Cell movement
1058 patterns during gastrulation in the chick are controlled by positive and
1059 negative chemotaxis mediated by FGF4 and FGF8. *Dev Cell* 3(3):425-437.
1060 6. Nomura S, *et al.* (2008) FGF10/FGFR2 signal induces cell migration and
1061 invasion in pancreatic cancer. *Br J Cancer* 99(2):305-313.
1062 7. Song S, *et al.* (2013) Pou5f1-dependent EGF expression controls E-cadherin
1063 endocytosis, cell adhesion, and zebrafish epiboly movements. *Dev Cell*
1064 24(5):486-501.
1065 8. Lu Z, Jiang G, Blume-Jensen P, & Hunter T (2001) Epidermal growth factor-
1066 induced tumor cell invasion and metastasis initiated by dephosphorylation
1067 and downregulation of focal adhesion kinase. *Mol Cell Biol* 21(12):4016-4031.
1068 9. Damm EW & Winklbauer R (2011) PDGF-A controls mesoderm cell
1069 orientation and radial intercalation during Xenopus gastrulation.
1070 *Development* 138(3):565-575.
1071 10. Jechlinger M, *et al.* (2006) Autocrine PDGFR signaling promotes mammary
1072 cancer metastasis. *J Clin Invest* 116(6):1561-1570.
1073 11. Mizoguchi T, Verkade H, Heath JK, Kuroiwa A, & Kikuchi Y (2008) Sdf1/Cxcr4
1074 signaling controls the dorsal migration of endodermal cells during zebrafish
1075 gastrulation. *Development* 135(15):2521-2529.
1076 12. Shen HB, Gu ZQ, Jian K, & Qi J (2013) CXCR4-mediated Stat3 activation is
1077 essential for CXCL12-induced cell invasion in bladder cancer. *Tumour Biol*
1078 34(3):1839-1845.

1079 13. Montero J-A, Kilian B, Chan J, Bayliss PE, & Heisenberg C-P (2003)
1080 Phosphoinositide 3-Kinase Is Required for Process Outgrowth and Cell
1081 Polarization of Gastrulating Mesendodermal Cells. *Current Biology*
1082 13(15):1279-1289.
1083 14. Wander SA*, et al.* (2013) PI3K/mTOR inhibition can impair tumor invasion
1084 and metastasis in vivo despite a lack of antiproliferative action in vitro:
1085 implications for targeted therapy. *Breast Cancer Res Treat* 138(2):369-381.
1086 15. Tsai WB, Zhang X, Sharma D, Wu W, & Kinsey WH (2005) Role of Yes kinase
1087 during early zebrafish development. *Dev Biol* 277(1):129-141.
1088 16. Barraclough J, Hodgkinson C, Hogg A, Dive C, & Welman A (2007) Increases in
1089 c-Yes Expression Level and Activity Promote Motility But Not Proliferation of
1090 Human Colorectal Carcinoma Cells. *Neoplasia* 9(9):745-IN732.
1091 17. Sharma D, Holets L, Zhang X, & Kinsey WH (2005) Role of Fyn kinase in
1092 signaling associated with epiboly during zebrafish development. *Dev Biol*
1093 285(2):462-476.
1094 18. Yadav V & Denning MF (2011) Fyn is induced by Ras/PI3K/Akt signaling and
1095 is required for enhanced invasion/migration. *Mol Carcinog* 50(5):346-352.
1096 19. Krens SF*, et al.* (2008) Distinct functions for ERK1 and ERK2 in cell migration
1097 processes during zebrafish gastrulation. *Dev Biol* 319(2):370-383.
1098 20. Radtke S, Milanovic M, & Rossé C (2013) ERK2 but not ERK1 mediates HGF-
1099 induced motility in non-small cell lung carcinoma cell lines. *J Cell Sci.*
1100 126(Pt11):2381-2391.
1101 21. Jopling C, van Geemen D, & den Hertog J (2007) Shp2 knockdown and
1102 Noonan/LEOPARD mutant Shp2-induced gastrulation defects. *PLoS Genet*
1103 3(12):e225.
1104 22. Wang FM*, et al.* (2005) SHP-2 promoting migration and metastasis of MCF-7
1105 with loss of E-cadherin, dephosphorylation of FAK and secretion of MMP-9
1106 induced by IL-1beta in vivo and in vitro. *Breast Cancer Res Treat* 89(1):5-14.
1107 23. Ip YT & Gridley T (2002) Cell movements during gastrulation: snail
1108 dependent and independent pathways. *Curr Opin Genet Dev* 12(4):423-429.
1109 24. Batlle E, Sancho E, Francí C, Domínguez D, & Monfar M (2000) The
1110 transcription factor snail is a repressor of E-cadherin gene expression in
1111 epithelial tumour cells. *Nat Cell Biol* 2(2):84-89.
1112 25. Shi J, Severson C, Yang J, Wedlich D, & Klymkowsky MW (2011) Snail2
1113 controls mesodermal BMP/Wnt induction of neural crest. *Development*
1114 138(15):3135-3145.
1115 26. Castanon I & Baylies MK (2002) A Twist in fate: evolutionary comparison of
1116 Twist structure and function. *Gene* 287(1-2):11-22.
1117 27. Yang J*, et al.* (2004) Twist, a master regulator of morphogenesis, plays an
1118 essential role in tumor metastasis. *Cell* 117(7):927-939.
1119 28. Fernando RI*, et al.* (2010) The T-box transcription factor Brachyury
1120 promotes epithelial-mesenchymal transition in human tumor cells. *J Clin*
1121 *Invest* 120(2):533-544.
1122 29. Vannier C, Mock K, Brabletz T, & Driever W (2013) Zeb1 regulates E-cadherin
1123 and Epcam (epithelial cell adhesion molecule) expression to control cell
1124 behavior in early zebrafish development. *J Biol Chem* 288(26):18643-18659.
1125 30. Spaderna S*, et al.* (2008) The transcriptional repressor ZEB1 promotes
1126 metastasis and loss of cell polarity in cancer. *Cancer Res* 68(2):537-544.
1127 31. Sander V, Reversade B, & De Robertis EM (2007) The opposing homeobox
1128 genes Goosecoid and Vent1/2 self-regulate Xenopus patterning. *EMBO J*
1129 26(12):2955-2965.
1130 32. Hartwell KA*, et al.* (2006) The Spemann organizer gene, Goosecoid, promotes
1131 tumor metastasis. *Proc Natl Acad Sci U S A* 103(50):18969-18974.

1132 33. Wilm B, James RG, Schultheiss TM, & Hogan BL (2004) The forkhead genes,
1133 Foxc1 and Foxc2, regulate paraxial versus intermediate mesoderm cell fate.
1134 *Dev Biol* 271(1):176-189.
1135 34. Mani SA, *et al.* (2007) Mesenchyme Forkhead 1 (FOXC2) plays a key role in
1136 metastasis and is associated with aggressive basal-like breast cancers. *Proc*
1137 *Natl Acad Sci U S A* 104(24):10069-10074.
1138 35. Miyagi C, *et al.* (2004) STAT3 noncell-autonomously controls planar cell
1139 polarity during zebrafish convergence and extension. *J Cell Biol* 166(7):975-
1140 981.
1141 36. Abdulghani J, *et al.* (2008) Stat3 promotes metastatic progression of prostate
1142 cancer. *Am J Pathol* 172(6):1717-1728.
1143 37. Lachnit M, Kur E, & Driever W (2008) Alterations of the cytoskeleton in all
1144 three embryonic lineages contribute to the epiboly defect of Pou5f1/Oct4
1145 deficient MZspg zebrafish embryos. *Dev Biol* 315(1):1-17.
1146 38. Dai X, *et al.* (2013) OCT4 regulates epithelial-mesenchymal transition and its
1147 knockdown inhibits colorectal cancer cell migration and invasion. *Oncol Rep*
1148 29(1):155-160.
1149 39. O'Carroll D, *et al.* (2001) The polycomb-group gene Ezh2 is required for early
1150 mouse development. *Mol Cell Biol* 21(13):4330-4336.
1151 40. Ren G, *et al.* (2012) Polycomb protein EZH2 regulates tumor invasion via the
1152 transcriptional repression of the metastasis suppressor RKIP in breast and
1153 prostate cancer. *Cancer Res* 72(12):3091-3104.
1154 41. Lin F, *et al.* (2005) Essential roles of G{alpha}12/13 signaling in distinct cell
1155 behaviors driving zebrafish convergence and extension gastrulation
1156 movements. *J Cell Biol* 169(5):777-787.
1157 42. Chen MW, *et al.* (2010) H3K9 histone methyltransferase G9a promotes lung
1158 cancer invasion and metastasis by silencing the cell adhesion molecule Ep-
1159 CAM. *Cancer Res* 70(20):7830-7840.
1160 43. van der Lugt NM, *et al.* (1994) Posterior transformation, neurological
1161 abnormalities, and severe hematopoietic defects in mice with a targeted
1162 deletion of the bmi-1 proto-oncogene. *Genes Dev* 8(7):757-769.
1163 44. Guo BH, *et al.* (2011) Bmi-1 promotes invasion and metastasis, and its
1164 elevated expression is correlated with an advanced stage of breast cancer.
1165 *Mol Cancer* 10(1):10.
1166 45. Zhu S, Liu L, Korzh V, Gong Z, & Low BC (2006) RhoA acts downstream of
1167 Wnt5 and Wnt11 to regulate convergence and extension movements by
1168 involving effectors Rho kinase and Diaphanous: use of zebrafish as an in vivo
1169 model for GTPase signaling. *Cell Signal* 18(3):359-372.
1170 46. Yoshioka K, Nakamori S, & Itoh K (1999) Overexpression of small GTP-
1171 binding protein RhoA promotes invasion of tumor cells. *Cancer Res*
1172 59(8):2004-2010.
1173 47. Choi SC & Han JK (2002) Xenopus Cdc42 regulates convergent extension
1174 movements during gastrulation through Wnt/Ca2+ signaling pathway. *Dev*
1175 *Biol* 244(2):342-357.
1176 48. Reymond N, *et al.* (2012) Cdc42 promotes transendothelial migration of
1177 cancer cells through beta1 integrin. *J Cell Biol* 199(4):653-668.
1178 49. Habas R, Dawid IB, & He X (2003) Coactivation of Rac and Rho by
1179 Wnt/Frizzled signaling is required for vertebrate gastrulation. . *Genes Dev*
1180 17(2):295-309.
1181 50. Vega FM & Ridley AJ (2008) Rho GTPases in cancer cell biology. *FEBS Lett*
1182 582(14):2093-2101.

1183 51. Marlow F, Topczewski J, Sepich D, & Solnica-Krezel L (2002) Zebrafish Rho
1184 kinase 2 acts downstream of Wnt11 to mediate cell polarity and effective
1185 convergence and extension movements. *Curr Biol* 12(11):876-884.
1186 52. Itoh K, *et al.* (1999) An essential part for Rho-associated kinase in the
1187 transcellular invasion of tumor cells. *Nat Med* 5(2):221-225.
1188 53. Kusakabe M & Nishida E (2004) The polarity-inducing kinase Par-1 controls
1189 Xenopus gastrulation in cooperation with 14-3-3 and aPKC. *EMBO J*
1190 23(21):4190-4201.
1191 54. Shi X, Gangadharan B, Brass LF, Ruf W, & Mueller BM (2004) Protease-
1192 activated receptors (PAR1 and PAR2) contribute to tumor cell motility and
1193 metastasis. *Mol Cancer Res* 2(7):395-402.
1194 55. Gunaratne A, Thai BL, & Di Guglielmo GM (2013) Atypical protein kinase C
1195 phosphorylates Par6 and facilitates transforming growth factor beta-induced
1196 epithelial-to-mesenchymal transition. *Mol Cell Biol* 33(5):874-886.
1197 56. Seifert K, Ibrahim H, Stodtmeister T, Winklbauer R, & Niessen CM (2009) An
1198 adhesion-independent, aPKC-dependent function for cadherins in
1199 morphogenetic movements. *J Cell Sci* 122(Pt 14):2514-2523.
1200 57. Yamazaki K, *et al.* (2009) Adenylate cyclase-associated protein 1
1201 overexpressed in pancreatic cancers is involved in cancer cell motility. *Lab*
1202 *Invest* 89(4):425-432.
1203 58. Link V, *et al.* (2006) Identification of regulators of germ layer morphogenesis
1204 using proteomics in zebrafish. *J Cell Sci* 119(Pt 10):2073-2083.
1205 59. Khanna C, *et al.* (2004) The membrane-cytoskeleton linker ezrin is necessary
1206 for osteosarcoma metastasis. *Nat Med* 10(2):182-186.
1207 60. Slanchev K, *et al.* (2009) The epithelial cell adhesion molecule EpCAM is
1208 required for epithelial morphogenesis and integrity during zebrafish epiboly
1209 and skin development. *PLoS Genet* 5(7):e1000563.
1210 61. Ni J, *et al.* (2012) Role of the EpCAM (CD326) in prostate cancer metastasis
1211 and progression. *Cancer Metastasis Rev* 31(3-4):779-791.
1212 62. Skalski M, Alfandari D, & Darribere T (1998) A key function for alphav
1213 containing integrins in mesodermal cell migration during Pleurodeles waltl
1214 gastrulation. *Dev Biol* 195(2):158-173.
1215 63. Felding-Habermann B (2003) Integrin adhesion receptors in tumor
1216 metastasis. *Clin Exp Metastasis* 20(3):203-213.
1217 64. Marsden M & DeSimone DW (2003) Integrin-ECM Interactions Regulate
1218 Cadherin-Dependent Cell Adhesion and Are Required for Convergent
1219 Extension in Xenopus. *Current Biology* 13(14):1182-1191.
1220 65. Malik G, *et al.* (2010) Plasma fibronectin promotes lung metastasis by
1221 contributions to fibrin clots and tumor cell invasion. *Cancer Res* 70(11):4327-
1222 4334.
1223 66. Bakkers J, *et al.* (2004) Has2 is required upstream of Rac1 to govern dorsal
1224 migration of lateral cells during zebrafish gastrulation. *Development*
1225 131(3):525-537.
1226 67. Kim HR, *et al.* (2004) Hyaluronan facilitates invasion of colon carcinoma cells
1227 in vitro via interaction with CD44. *Cancer Res* 64(13):4569-4576.
1228 68. Coyle RC, Latimer A, & Jessen JR (2008) Membrane-type 1 matrix
1229 metalloproteinase regulates cell migration during zebrafish gastrulation:
1230 evidence for an interaction with non-canonical Wnt signaling. *Exp Cell Res*
1231 314(10):2150-2162.
1232 69. Perentes JY, *et al.* (2011) Cancer cell-associated MT1-MMP promotes blood
1233 vessel invasion and distant metastasis in triple-negative mammary tumors.
1234 *Cancer Res* 71(13):4527-4538.

1235 70. Cha YI, *et al.* (2006) Cyclooxygenase-1-derived PGE2 promotes cell motility
1236 via the G-protein-coupled EP4 receptor during vertebrate gastrulation. *Genes*
1237 *Dev* 20(1):77-86.
1238 71. Kundu N & Fulton AM (2002) Selective cyclooxygenase (COX)-1 or COX-2
1239 inhibitors control metastatic disease in a murine model of breast cancer.
1240 *Cancer Res* 62(8):2343-2346.
1241 72. Speirs CK, *et al.* (2010) Prostaglandin Gbetagamma signaling stimulates
1242 gastrulation movements by limiting cell adhesion through Snai1a
1243 stabilization. *Development* 137(8):1327-1337.
1244 73. Wang D & Dubois RN (2006) Prostaglandins and cancer. *Gut* 55(1):115-122.
1245 74. Yamashita S, *et al.* (2004) Zinc transporter LIVI controls epithelial-
1246 mesenchymal transition in zebrafish gastrula organizer. *Nature*
1247 429(6989):298-302.
1248 75. Lue HW, *et al.* (2011) LIV-1 promotes prostate cancer epithelial-to-
1249 mesenchymal transition and metastasis through HB-EGF shedding and EGFR-
1250 mediated ERK signaling. *PLoS One* 6(11):e27720.
1251 76. Yagi H, *et al.* (2011) A synthetic biology approach reveals a CXCR4-G13-Rho
1252 signaling axis driving transendothelial migration of metastatic breast cancer
1253 cells. *Sci Signal* 4(191):ra60.
1254 77. Webster DM, *et al.* (2009) O-GlcNAc modifications regulate cell survival and
1255 epiboly during zebrafish development. *BMC Dev Biol* 9:28.
1256 78. Lynch TP, *et al.* (2012) Critical role of O-Linked beta-N-acetylglucosamine
1257 transferase in prostate cancer invasion, angiogenesis, and metastasis. *J Biol*
1258 *Chem* 287(14):11070-11081.
1259 79. Latinkic BV (2003) Xenopus Cyr61 regulates gastrulation movements and
1260 modulates Wnt signalling. *Development* 130(11):2429-2441.
1261 80. Lin J, *et al.* (2012) A novel anti-Cyr61 antibody inhibits breast cancer growth
1262 and metastasis in vivo. *Cancer Immunol Immunother* 61(5):677-687.
1263 81. Liu W, *et al.* (2011) TRPM7 regulates gastrulation during vertebrate
1264 embryogenesis. *Dev Biol* 350(2):348-357.
1265 82. Middelbeek J, *et al.* (2012) TRPM7 is required for breast tumor cell
1266 metastasis. *Cancer Res* 72(16):4250-4261.
1267 83. Holloway BA, *et al.* (2009) A novel role for MAPKAPK2 in morphogenesis
1268 during zebrafish development. *PLoS Genet* 5(3):e1000413.
1269 84. Kumar B, *et al.* (2010) p38 mitogen-activated protein kinase-driven
1270 MAPKAPK2 regulates invasion of bladder cancer by modulation of MMP-2
1271 and MMP-9 activity. *Cancer Res* 70(2):832-841.
1272 85. Machingo QJ, Fritz A, & Shur BD (2006) A beta1,4-galactosyltransferase is
1273 required for convergent extension movements in zebrafish. *Dev Biol*
1274 297(2):471-482.
1275 86. Zhu X, *et al.* (2005) Elevated beta1,4-galactosyltransferase I in highly
1276 metastatic human lung cancer cells. Identification of E1AF as important
1277 transcription activator. *J Biol Chem* 280(13):12503-12516.
1278 87. Hong SK, Tanegashima K, & Dawid IB (2011) XIer2 is required for convergent
1279 extension movements during Xenopus development. *Int J Dev Biol* 55(10-
1280 12):917-921.
1281 88. Neeb A, *et al.* (2012) The immediate early gene Ier2 promotes tumor cell
1282 motility and metastasis, and predicts poor survival of colorectal cancer
1283 patients. *Oncogene* 31(33):3796-3806.
1284 89. Besser J, Leito JT, van der Meer DL, & Bagowski CP (2007) Tip-1 induces
1285 filopodia growth and is important for gastrulation movements during
1286 zebrafish development. *Dev Growth Differ* 49(3):205-214.

1287 90. Han M, Wang H, Zhang HT, & Han Z (2012) The PDZ protein TIP-1 facilitates
1288 cell migration and pulmonary metastasis of human invasive breast cancer
1289 cells in athymic mice. *Biochem Biophys Res Commun* 422(1):139-145.
1290 91. Faure S, *et al.* (2005) Xenopus p21-activated kinase 5 regulates blastomeres'
1291 adhesive properties during convergent extension movements. *Dev Biol*
1292 277(2):472-492.
1293 92. Gong W, *et al.* (2009) P21-activated kinase 5 is overexpressed during
1294 colorectal cancer progression and regulates colorectal carcinoma cell
1295 adhesion and migration. *Int J Cancer* 125(3):548-555.
1296 93. Iioka H, Ueno N, & Kinoshita N (2004) Essential role of MARCKS in cortical
1297 actin dynamics during gastrulation movements. *J Cell Biol* 164(2):169-174.
1298 94. Rombouts K, *et al.* (2013) Myristoylated Alanine-Rich protein Kinase C
1299 Substrate (MARCKS) expression modulates the metastatic phenotype in
1300 human and murine colon carcinoma in vitro and in vivo. *Cancer Lett*
1301 333(2):244-252.
1302 95. Medici D, Hay ED, & B.R. O (2008) Snail and Slug Promote Epithelial-
1303 Mesenchymal Transition through -Catenin–T-Cell Factor-4-dependent Expression
1304 of Transforming Growth Factor-3. Molecular Biology of the Cell 19(11):4875–
1305 4887.
1306
1307
1308 **Legend for source data**

1309 **Figure 2a_HRT2C_source data**

1310 Western blot analysis of HRT2C protein levels in non-metastatic human cancer cell

1311 line, MCF7 (breast) and highly metastatic human cancer cell lines, MDA-MB-231

1312 (breast), MDA-MB-435 (melanoma), MIA-PaCa2 (pancreas), SW620 (colon) and

1313 PC3 (prostate).

1314

1315 **Figure 2a_GAPDH_source data**

1316 Western blot analysis of GAPDH protein levels in non-metastatic human cancer cell

1317 line, MCF7 (breast) and highly metastatic human cancer cell lines, MDA-MB-231

1318 (breast), MDA-MB-435 (melanoma), MIA-PaCa2 (pancreas), SW620 (colon) and

1319 PC3 (prostate).

1320

1321 **Figure 3C_E-cadherin in MCF7_ source data**

1322 Western blot analysis of HRT2C protein levels in MCF7 cells expressing either the

1323 control vector or HTR2C.

1324

1325 **Figure 3C_EpCAM in MCF7_ source data**

1326 Western blot analysis of EpCAM protein levels in MCF7 cells expressing either the

1327 control vector or HTR2C.

1328

1329 **Figure 3C_Vimentin in MCF7_ source data**

1330 Western blot analysis of Vimentin protein levels in MCF7 cells expressing either the

1331 control vector or HTR2C.

1332

1333 **Figure 3C_N-cadherin in MCF7_ source data**

1334 Western blot analysis of N-cadherin protein levels in MCF7 cells expressing either the

1335 control vector or HTR2C.

1336

1337 **Figure 3C_Zeb1 in MCF7_ source data**

1338 Western blot analysis of Zeb1 protein levels in MCF7 cells expressing either the

1339 control vector or HTR2C.

1340

1341 **Figure 3C_HRT2C in MCF7_ source data**

1342 Western blot analysis of HRT2C protein levels in MCF7 cells expressing either the

1343 control vector or HTR2C.

1344

1345 **Figure 3C_GAPDH in MCF7_source data**

1346 Western blot analysis of GAPDH protein levels in MCF7 cells expressing either the

1347 control vector or HTR2C.

1348

1349 **Figure 3C_E-cadherin in HaCaT_source data**

1350 Western blot analysis of E-cadherin protein levels in HaCaT cells expressing either
1351 the control vector or HTR2C.
1352
1353 **Figure 3C_EpCAM in HaCaT_source data**
1354 Western blot analysis of EpCAM protein levels in HaCaT cells expressing either the
1355 control vector or HTR2C.
1356
1357 **Figure 3C_Vimentin in HaCaT_source data**
1358 Western blot analysis of Vimentin protein levels in HaCaT cells expressing either the
1359 control vector or HTR2C.
1360
1361 **Figure 3C_Zeb1 in HaCaT_source data**
1362 Western blot analysis of zeb1 protein levels in HaCaT cells expressing either the
1363 control vector or HTR2C.
1364
1365 **Figure 3C_HRT2C in HaCaT_source data**
1366 Western blot analysis of HRT2C protein levels in HaCaT cells expressing either the
1367 control vector or HTR2C.
1368
1369 **Figure 3C_GAPDH in HaCaT_source data**
1370 Western blot analysis of GAPDH protein levels in HaCaT cells expressing either the
1371 control vector or HTR2C.
1372
1373 **Figure 5C_E-cadherin_source data**
1374 Western blot analysis of E-cadherin protein levels in whole cell lysate of 4T1 primary
1375 tumors from either vehicle or Pizotifen-treated mice.

1376

1377 **Figure 5C_Zeb1 _source data**

1378 Western blot analysis of Zeb1 protein levels in whole cell lysate of 4T1 primary

1379 tumors from either vehicle or Pizotifen-treated mice.

1380

1381 **Figure 5C_ Phosphorylation of serine-9 in GSK3β_source data**

1382 Western blot analysis of the protein levels of phosphorylation of serine-9 in GSK3β in

1383 whole cell lysate of 4T1 primary tumors from either vehicle or Pizotifen-treated mice.

1384

1385 **Figure 5C_ GSK3β_source data**

1386 Western blot analysis of GSK3β protein levels in whole cell lysate of 4T1 primary

1387 tumors from either vehicle or Pizotifen-treated mice.

1388

1389 **Figure 5C_Luciferase_source data**

1390 Western blot analysis of Luciferase protein levels in whole cell lysate of 4T1 primary

1391 tumors from either vehicle or Pizotifen-treated mice.

1392

1393 **Figure 5C_β-catenin in the nucleus_source data**

1394 Western blot analysis of β-catenin protein levels in the nucleus of 4T1 primary tumors

1395 from either vehicle or Pizotifen-treated mice.

1396

1397 **Figure 5C_Histone H3 in the nucleus_source data**

1398 Western blot analysis of Histone H3 protein levels in the nucleus of 4T1 primary

1399 tumors from either vehicle or Pizotifen-treated mice.

1400

1401 **Figure 5C_β-catenin in the cytoplasm_source data**

1402 Western blot analysis of β-catenin protein levels in the cytoplasm of 4T1 primary
1403 tumors from either vehicle or Pizotifen-treated mice.
1404
1405 **Figure 5C_β-tubulin in the cytoplasm_source data**
1406 Western blot analysis of β-tubulin protein levels in the cytoplasm of 4T1 primary
1407 tumors from either vehicle or Pizotifen-treated mice.
1408
1409 **Figure 5D_E-cadherin_source data**
1410 Western blot analysis of E-cadherin protein levels in either vehicle or Pizotifen-treated
1411 MDA-MB-231 cells or E-cadherin positive cells in Pizotifen-treated MDA-MB-231
1412 cells.
1413
1414 **Figure 5D_EpCAM_source data**
1415 Western blot analysis of EpCAM protein levels in either vehicle or Pizotifen-treated
1416 MDA-MB-231 cells or E-cadherin positive cells in Pizotifen-treated MDA-MB-231
1417 cells.
1418
1419 **Figure 5D_Keratin18 (KRT18)_source data**
1420 Western blot analysis of KRT18 protein levels in either vehicle or Pizotifen-treated
1421 MDA-MB-231 cells or E-cadherin positive cells in Pizotifen-treated MDA-MB-231
1422 cells.
1423
1424 **Figure 5D_Keratin19 (KRT19)_source data**
1425 Western blot analysis of KRT19 protein levels in either vehicle or Pizotifen-treated
1426 MDA-MB-231 cells or E-cadherin positive cells in Pizotifen-treated MDA-MB-231
1427 cells.

1428

1429 **Figure 5D_Vimentin_source data**

1430 Western blot analysis of Vimentin protein levels in either vehicle or Pizotifen-treated

1431 MDA-MB-231 cells or E-cadherin positive cells in Pizotifen-treated MDA-MB-231

1432 cells.

1433

1434 **Figure 5D_MMP1_source data**

1435 Western blot analysis of MMP1 protein levels in either vehicle or Pizotifen-treated

1436 MDA-MB-231 cells or E-cadherin positive cells in Pizotifen-treated MDA-MB-231

1437 cells.

1438

1439 **Figure 5D_MMP3_source data**

1440 Western blot analysis of MMP3 protein levels in either vehicle or Pizotifen-treated

1441 MDA-MB-231 cells or E-cadherin positive cells in Pizotifen-treated MDA-MB-231

1442 cells.

1443

1444 **Figure 5D_S100A4_source data**

1445 Western blot analysis of S100A4 protein levels in either vehicle or Pizotifen-treated

1446 MDA-MB-231 cells or E-cadherin positive cells in Pizotifen-treated MDA-MB-231

1447 cells.

1448

1449 **Figure 5D_Zeb1_source data**

1450 Western blot analysis of Zeb1 protein levels in either vehicle or Pizotifen-treated

1451 MDA-MB-231 cells or E-cadherin positive cells in Pizotifen-treated MDA-MB-231

1452 cells.

1453

1454 **Figure 5D_GAPDH_source data**

1455 Western blot analysis of GAPDH protein levels in either vehicle or Pizotifen-treated
1456 MDA-MB-231 cells or E-cadherin positive cells in Pizotifen-treated MDA-MB-231
1457 cells.

1458

1459 **Figure 5F_β-catenin in the nucleus_source data**

1460 Western blot analysis of β-catenin protein levels in the nuclear of MCF7 cells
1461 expressing either the control vector or HTR2C.

1462

1463 **Figure 5F_Histone H3 in the nucleus _source data**

1464 Western blot analysis of Histone H3 protein levels in the nuclear of MCF7 cells
1465 expressing either the control vector or HTR2C.

1466

1467 **Figure 5F_β-catenin in the cytoplasm_source data**

1468 Western blot analysis of β-catenin protein levels in the cytoplasm of MCF7 cells
1469 expressing either the control vector or HTR2C.

1470

1471 **Figure 5F_β-tubulin in the cytoplasm_source data**

1472 Western blot analysis of β-tubulin protein levels in the cytoplasm of MCF7 cells
1473 expressing either the control vector or HTR2C.

1474

1475 **Figure 5F_Phosphorylation of serine-9 in GSK3β_source data**

1476 Western blot analysis of the protein levels of phosphorylation of serine-9 in GSK3β in
1477 whole cell lysate of MCF7 cells expressing either the control vector or HTR2C.

1478

1479 **Figure 5F_GSK3β_source data**

1480 Western blot analysis of GSK3β protein levels in whole cell lysate of MCF7 cells
1481 expressing either the control vector or HTR2C.
1482
1483 **Figure 5F_GAPDH_source data**
1484 Western blot analysis of GAPDH protein levels in whole cell lysate of MCF7 cells
1485 expressing either the control vector or HTR2C.
1486
1487 **Figure 5H_β-catenin in the nucleus_source data**
1488 Western blot analysis of β-catenin protein levels in the nucleus of either vehicle or
1489 Pizotifen-treated MDA-MB-231 cells or E-cadherin positive cells in Pizotifen-treated
1490 MDA-MB-231 cells.
1491
1492 **Figure 5H_Histone H3 in the nucleus _source data**
1493 Western blot analysis of Histone H3 protein levels in the nucleus of either vehicle or
1494 Pizotifen-treated MDA-MB-231 cells or E-cadherin positive cells in Pizotifen-treated
1495 MDA-MB-231 cells.
1496
1497 **Figure 5H_β-catenin in the cytoplasm_source data**
1498 Western blot analysis of β-catenin protein levels in the cytoplasm of either vehicle or
1499 Pizotifen-treated MDA-MB-231 cells or E-cadherin positive cells in Pizotifen-treated
1500 MDA-MB-231 cells.
1501
1502 **Figure 5H_β-tubulin in the cytoplasm_source data**
1503 Western blot analysis of β-tubulin protein levels in the cytoplasm of either vehicle or
1504 Pizotifen-treated MDA-MB-231 cells or E-cadherin positive cells in Pizotifen-treated
1505 MDA-MB-231 cells.

1506

1507 **Figure 5H_Phosphorylation of serine-9 in GSK3β_source data**

1508 Western blot analysis of the protein levels of phosphorylation of serine-9 in GSK3β in

1509 whole cell lysate of either vehicle or Pizotifen-treated MDA-MB-231 cells or E-

1510 cadherin positive cells in Pizotifen-treated MDA-MB-231 cells.

1511

1512 **Figure 5H_GSK3β_source data**

1513 Western blot analysis of GSK3β protein levels in whole cell lysate of either vehicle or

1514 Pizotifen-treated MDA-MB-231 cells or E-cadherin positive cells in Pizotifen-treated

1515 MDA-MB-231 cells.

1516

1517 **Figure 5H_GAPDH_source data**

1518 Western blot analysis of GSK3β protein levels in whole cell lysate of either vehicle or

1519 Pizotifen-treated MDA-MB-231 cells or E-cadherin positive cells in Pizotifen-treated

1520 MDA-MB-231 cells.

1521

1522 **Figure S1A_ PRMT1_source data**

1523 Western blot analysis of PRMT1 protein levels in non-metastatic human cancer cell

1524 line (MCF7) and highly metastatic human cancer cell lines (MDA-MB-231, MDA-

1525 MB-435, MIA-PaCa2, PC9, HCCLM3, SW620 and PC3).

1526

1527 **Figure S1A_ CYP11A1_source data**

1528 Western blot analysis of CYP11A1 protein levels in non-metastatic human cancer cell

1529 line (MCF7) and highly metastatic human cancer cell lines (MDA-MB-231, MDA-

1530 MB-435, MIA-PaCa2, PC9, HCCLM3, SW620 and PC3).

1531

1532 **Figure S1A_ β-actin_source data**

1533 Western blot analysis of β-actin protein levels in non-metastatic human cancer cell

1534 line (MCF7) and highly metastatic human cancer cell lines (MDA-MB-231, MDA-

1535 MB-435, MIA-PaCa2, PC9, HCCLM3, SW620 and PC3).

1536

1537 **Figure S1A_ PRMT1_source data**

1538 Western blot analysis of PRMT1 protein levels in sub-clones of MBA-MB-231 cells

1539 which were transfected with either a control shRNA targeting LacZ or one of four

1540 independent shRNAs targeting PRMT1 (clone #1 to #4).

1541

1542 **Figure S1A_ β-actin _source data**

1543 Western blot analysis of β-actin protein levels in sub-clones of MBA-MB-231 cells

1544 which were transfected with either a control shRNA targeting LacZ or one of four

1545 independent shRNAs targeting PRMT1 (clone #1 to #4).

1546

1547 **Figure S1A_CYP11A1_source data**

1548 Western blot analysis of CYP11A1 protein levels in sub-clones of MBA-MB-231

1549 cells which were transfected with either a control shRNA targeting LacZ or one of

1550 four independent shRNAs targeting CYP11A1 (clone #1 to #4).

1551

1552 **Figure S1A_ β-actin_source data**

1553 Western blot analysis of β-actin protein levels in sub-clones of MBA-MB-231 cells

1554 which were transfected with either a control shRNA targeting LacZ or one of four

1555 independent shRNAs targeting CYP11A1 (clone #1 to #4).

1556

1557 **Figure S2A_DRD2_source data**

1558 Western blot analysis of DRD2 protein levels in non-metastatic human cancer cell
1559 line, MCF7 (breast) and highly metastatic human cancer cell lines, MDA-MB-231
1560 (breast), MDA-MB-435 (melanoma), MIA-PaCa2 (pancreas), PC3 (prostate) and
1561 SW620 (colon)
1562
1563 **Figure S2A_GAPDH_source data**
1564 Western blot analysis of GAPDH protein levels in non-metastatic human cancer cell
1565 line, MCF7 (breast) and highly metastatic human cancer cell lines, MDA-MB-231
1566 (breast), MDA-MB-435 (melanoma), MIA-PaCa2 (pancreas), PC3 (prostate) and
1567 SW620 (colon)